

3-23-2018

Characterization of ATD And Human Responses To -Gz Accelerative Input

Joe R. Berry

Follow this and additional works at: <https://scholar.afit.edu/etd>

Recommended Citation

Berry, Joe R., "Characterization of ATD And Human Responses To -Gz Accelerative Input" (2018). *Theses and Dissertations*. 1874.
<https://scholar.afit.edu/etd/1874>

This Thesis is brought to you for free and open access by the Student Graduate Works at AFIT Scholar. It has been accepted for inclusion in Theses and Dissertations by an authorized administrator of AFIT Scholar. For more information, please contact richard.mansfield@afit.edu.



CHARACTERIZATION OF ATD AND HUMAN RESPONSES TO -GZ
ACCELERATIVE INPUT

THESIS

Joe R. Berry, Captain, USAF

AFIT-ENV-MS-18-M-178

DEPARTMENT OF THE AIR FORCE
AIR UNIVERSITY

AIR FORCE INSTITUTE OF TECHNOLOGY

Wright-Patterson Air Force Base, Ohio

DISTRIBUTION STATEMENT A. APPROVED FOR PUBLIC RELEASE;
DISTRIBUTION UNLIMITED

The views expressed in this thesis are those of the author and do not reflect the official policy or position of the United States Air Force, Department of Defense, or the U.S. Government. This material is declared a work of the U.S. Government and is not subject to copyright protection in the United States.

AFIT-ENV-MS-18-M-178

CHARACTERIZATION OF ATD AND HUMAN RESPONSES TO -GZ
ACCELERATIVE INPUT

THESIS

Presented to the Faculty

Department of Systems Engineering and Management

Graduate School of Engineering and Management

Air Force Institute of Technology

Air University

Air Education and Training Command

In Partial Fulfillment of the Requirements for the
Degree of Master of Science in Systems Engineering

Joe R. Berry, MS

Captain, USAF

March 2018

DISTRIBUTION STATEMENT A. APPROVED FOR PUBLIC RELEASE;
DISTRIBUTION UNLIMITED

CHARACTERIZATION OF ATD AND HUMAN RESPONSES TO -GZ
ACCELERATIVE INPUT

Joe R. Berry, MS
Captain, USAF

Committee Membership:

Jeffrey C. Parr, PhD, Lt Col, USAF
Chair

Michael E. Miller, PhD
Member

John Buhrman, MS
Member

Abstract

Modern Helmet Mounted Displays (HMD) provide pilots with capabilities that are essential in today's advanced military operating environment but come at the cost of additional head supported mass at a mechanically disadvantaged position. Additionally, the United States Air Force's (USAF) expanded range of accepted pilot size increases the risk for neck injuries during ejection. This increased risk of injury drove Parr (2014) to develop a human-data based neck injury criteria, called the MANIC, that improves objective interpretation of ejection system test results and provides early input to HMD and escape system design. The criteria's risk functions provide the ability to limit risk of AIS 2+ and AIS 3+ injury below 5%. All USAF ejection system proof of concept and full system developmental testing uses Anthropometric Test Developments (ATD). However, biomechanical differences observed between human and ATD MANIC responses necessitate a conversion between ATD and human risk functions before utilizing ATD responses to evaluate risk of injury given the human MANIC criteria. This research creates a transfer function for the MANIC(-Gz) responses using linear regression and makes the previously developed human-based neck injury criterion directly applicable to accelerative testing with ATDs.

The resulting proportional difference between the regression models defined the transfer function between human and ATD responses. Parametric survival analysis for transformed human tensile neck loads produced ATD injury risk curves for AIS 2+ and AIS 3+ injury. The ATD AIS 2+ risk curve shows a 5% probability of injury at 380.9 N (95% CI 268.30 N, 493.6 N). The ATD AIS 3+ risk curve shows a 5% probability of injury at 418.8 N (95% CI 297.4 N, 540.3 N). The difference in both sets of values and differs significantly from the previously developed human-data based limit of 1313 N for AIS 2+ and 1462 N for AIS 3+.

Acknowledgments

Thank you to my thesis advisor for your guidance, encouragement, and mentorship during my time at AFIT.

Thank you to my wife for your time, energy, and patience throughout my graduate program and thesis work.

Joe R. Berry

Table of Contents

	Page
Abstract	iv
Acknowledgments.....	v
Table of Contents	vi
List of Figures	ix
List of Tables	xi
I. Introduction	1
General Issue.....	1
Problem Statement	1
Justification/Expected Contributions	3
Assumptions/Limitations	4
Nature of the Study	4
Summary	5
II. Literature Review	6
Introduction.....	6
MANIC	7
MIL-HDBK-516CN-5b	10
Ejection Events	10
Anatomical Axes and Points of Reference	13
AIS 2 and 3 – Injury Classification.....	14
Lack of Data.....	15
Rocket Sled Tests.....	16

Laboratory Tests	17
ATD Testing	18
PMHS Testing.....	19
Fuller Envelope – New Air Force Body Types Accepted	20
Transfer Function.....	21
Risk Curve for ATDs	23
III. Methodology.....	24
Introduction.....	24
Original Data Source.....	24
Assigning Accelerative Loads to PMHS Data Points.....	27
Linear Regression	27
Transfer Function.....	28
Survival Analysis	28
IV. Results	30
Overview.....	30
Assigning Accelerative Levels to PMHS Data Points.....	30
-Gx Tensile Neck Load Transfer Function	33
95% Confidence Intervals of Linear Models used in -Gx Transfer Functions	38
-Gz Tensile Neck Load Transfer Function	40
95% Confidence Intervals of Linear Models used in -Gz Transfer Functions	45
Equivalent ATD Tensile Neck Load Values	47
Hybrid III 50th Automotive Manikin ATD AIS 2+ and 3+ Risk Curves.....	47
Exclusion of PMHS Data from (-Gx) Accelerative Studies	48

AIS 2+ MANIC(-Gz) Risk Curves Using Transfer Function 95% Confidence Bounds	50
.....	
AIS 3+ MANIC(-Gz) Risk Curves Using Transfer Function 95% Confidence Bounds	52
.....	
V. Conclusions and Recommendations	54
Research Purpose and Goals	54
Investigative Questions Answered	54
Recommendations for Future Work	59
Appendix A: Live Human Data from -Gz Accelerative Studies Used in Creating -Gz Transfer Function	61
Appendix B: Computer Code to Convert Human/PMHS (-Gz) and (-Gx) Data to Equivalent ATD Data and Perform Survival Analysis	66
Bibliography	69

List of Figures

	Page
Figure 1. Overview of ATD to Human Transfer Function Implementation.....	7
Figure 2. Overview of Development of the MANIC's Risk Functions.....	9
Figure 3. Acceleration Axes (Parr, 2014).....	13
Figure 4. Laboratory Acceleration Test Subject Equipped with Bite-bar Accelerometer	15
Figure 5. Side-by-side Comparison of ATD and Human Spinal Structures.....	19
Figure 6. Difference in Head/Neck Response to Similar GY Accelerative Input (Satava, 2017).....	22
Figure 7. Seat Accelerometers on Mounting Bracket, (Specker and Plaga, 1996).....	31
Figure 8. Test Number 11, 694 KEAS, Four Seat Accelerometer Data (Specker and Plaga, 1996).....	32
Figure 9. Linear Regression of Human and ATD (-Gx) Tensile Data and (-Gx) Transfer Function.....	37
Figure 10. -Gx Tensile Neck Load Linear Regression Models and 95% Confidence Interval Bounds.....	39
Figure 11. Corrected Human-based Risk Curves for Probability of Abbreviated Injury Scale (AIS) 2+ and 3+.....	42
Figure 12. Linear Regression of Human and ATD (-Gz) Tensile Data and (-Gz) Transfer Function.....	44
Figure 13. -Gz Linear Regression Models and 95% Confidence Interval Bounds.....	45
Figure 14. -Gz Transfer Function Based on Most Conservative Linear Models.....	46
Figure 15. -Gz Transfer Function Based on Least Conservative Linear Models.....	46

Figure 16. ATD-based Risk Curve Probability of Abbreviated Injury Scale (AIS) 2+ and 3+ after Use of -Gz Tensile Neck Load Transfer Function	48
Figure 17. Excluding -Gx PMHS Accelerative Study Data ATD-based Risk Curve Probability of Abbreviated Injury Scale (AIS) 3+ after Use of -Gz Transfer Function	49
Figure 18. 5% Probability of AIS 2+ Injury After Converting Data Using Most Likely Value and 95% Confidence Interval Bounds for the Transfer Functions	50
Figure 19. 5% Probability of AIS 3+ Injury After Converting Data Using Most Likely Value and 95% Confidence Interval Bounds for the Transfer Functions	52
Figure 20. Most Likely Value for the Tensile Neck Load Transfer Function for -Gz Accelerative Input	56
Figure 21. More Conservative Value for the Tensile Neck Load Transfer Function for -Gz Accelerative Input	56
Figure 22. Less Conservative Value for the Tensile Neck Load Transfer Function for -Gz Accelerative Input	57
Figure 23. ATD-based Risk Curve Probability of Abbreviated Injury Scale (AIS) 3+ after Use of Most Likely Value of Transfer Functions	58

List of Tables

	Page
Table 1. MANIC Summary (Parr, 2014)	8
Table 2. X, Y, and Z Axial Components of the MANIC.....	10
Table 3. Test Number 11, 694 KEAS, Test Parameters. (Specker and Plaga, 1996).....	31
Table 4. Test Number 11, 694 KEAS, Ejection Sequence Timing (Specker and Plaga, 1996).....	31
Table 5. Test Number 11, 694 KEAS, Seat Accelerations. (Specker and Plaga, 1996)...	31
Table 6. Human Data from -Gx Accelerative Studies Used in Creating -Gx Transfer Function	34
Table 7. PMHS Data from -Gx Accelerative Studies Used in Creating -Gx Transfer Function	35
Table 8. ATD Data from -Gx Accelerative Studies Used in Creating -Gx Transfer Function	36
Table 9. PMHS Data from -Gz Accelerative Studies Used in Creating -Gz Tensile Neck Load Transfer Function.....	40
Table 10. ATD Data from -Gz Accelerative Studies Used in Creating -Gz Transfer Function	43
Table 11. Most Likely and 95% CI Values of Tensile Neck Load Values Corresponding to the Presented Transfer Functions and the 5% Probability of AIS 2+ Injury	51
Table 12. Most Likely and 95% CI Values of Tensile Neck Load Values Corresponding to the Presented Transfer Functions and the 5% Probability of AIS 3+ Injury	53

Characterization of ATD and Human Responses Under -Gz Accelerative Input

I. Introduction

General Issue

Determining the risk of neck injury in United States Air Force (USAF) pilots during ejection events is difficult yet increasingly important as newly advanced technologies add weight to helmets and as the accepted range of pilot weights have been increased to include both smaller pilots with weights as low as 103 lbs as well as larger pilots having weights as high as 246 lbs (Nichols, 2006). During the USAF acquisition process, ejection seats, HMDs, and other escape system components are tested in full-up ejection event tests in combination with a human surrogate, known as an Anthropometric Test Device (ATD), which is subjected to the dynamic accelerative loading experienced during the full sequence of ejection. The ATD's neck loads are observed throughout the duration of the ejection and are used to compute peak values of the Multi-Axial Neck Injury Criteria's (MANIC) X, Y, and Z-axis components (referred to as MANIC by Parr) (Parr, 2014; Draft EZFC-CSB-16-001, 2017). The peak values are compared to the acceptable risk metrics as defined by the Air Force Life Cycle Management Center (AFLCMC) to ensure the system is acceptably safe.

Problem Statement

Despite significant biofidelic differences between humans and ATDs, current military standard MIL-HDBK-516CN-5 applies human-data based MANIC to ATD data during full-up ejection tests. The biofidelic differences refer to differences in ATD neck and human neck response in highly accelerative environments. Thus, the problem is that the ATD data may be either consistently more conservative, thus constraining the design of escape system components,

or less conservative, putting pilots at greater neck injury risk than desired. However, the assumption that the ATD's neck responses are representative of a human's neck response is inherent in the current testing standards' application.

This research will analyze previously collected data including Hybrid III and human/cadaver neck loads under z-axis laboratory acceleration levels to develop a mathematical relationship (hereafter referred to as a transfer function) between the two data sets. This research will explore the necessity and development of such a transfer function for $-G_z$ (tensile upper neck loading). The transfer function would then be applied to ATD data collected during future system verification tests to estimate the likely human loads and to apply the estimate to the calculation of the MANIC value. If a human to ATD transfer function is created, the MANIC can be applied to ATD data with improved confidence. Zinck (2016) and Satava (2017) furthered the MANIC implementation by demonstrating proofs of concept for an ATD to human transfer function of MANIC(-G_x) and MANIC(G_y) responses, the x-axis and y-axis components of the MANIC respectively.

This research is follow-on research and seeks to expand on the efforts of Parr et al. (2014), Zinck (2016), and Satava (2017) by developing ATD response correlations under G_z accelerative input for use with MANIC(G_z) implementation. In doing so, the following investigative questions will be addressed:

- What is the difference in tensile neck load response between human/PMHS and Hybrid III 50th Automotive Manikin ATDs over the operational range of accelerative input?
- Are human and ATD neck load responses significantly different and does the difference justify the need for a transfer function?

- What is an appropriate transfer function for making human-based -Gz risk functions, developed by Parr (2014), and associated neck injury criterion more appropriate for ejection system testing with ATDs?

- If a transfer function is appropriate, what is the equivalent ATD MANIC(-Gz) risk curve that would provide an equivalent 5% probability of AIS 2+ and 3+ injury for ATD tensile neck loads during ejection tests?

Justification/Expected Contributions

With the ability to accurately predict the probability of pilot neck injury during ejection events, the USAF would be able to fully explore the design space of new technology such as the Helmet Mounted Display (HMD) which adds capabilities and improves the performance of the pilots. Without that ability, the USAF would be forced to design HMDs as conservatively as possible or forego their use entirely. When the subjects wear an HMD (as compared to when the subjects do not wear one), those studies have shown significant increases in forces and moments in the neck, summarily referred to as neck loads, which directly drive an increase of the risk of neck injury (Buhrman and Perry, 1994; Perry, 1998; Doczy, Mosher, and Buhrman, 2004).

The current neck injury criteria, MANIC, is limited in its application to ATDs without a transfer function. This research will directly translate ATD neck load results to the probability of human injury by using the associated injury criteria used during safety testing of aircraft ejection systems in -Gz accelerative loading. Additionally, this research will be applicable to any domain where occupants experience high acceleration environments such as in collisions of ground vehicles.

Assumptions/Limitations

In the development of a transfer function for each of the three axes, the assumption is made that all neck loads are independent such that there is no interaction between neck load forces and moments in predicting neck injury. This research is limited by the available PMHS data in that the independent variable from the study with the largest sample size ($n = 12$) is tensile neck load and there is no associated accelerative load, only a pulse of tension was applied to generate injury in the PMHS (Parr et. al., 2014; Ylienimi, et. al., 2009). Therefore, an equivalent accelerative load will have to be extrapolated from the available data or those data points will be unavailable for creating the transfer function. Because tensile neck load is the only shared data point between the available z-axis data, this research (and the z-axis component of MANIC), assumes that tensile neck load is the only significant predictor of neck injury risk during acceleration along the z-axis. This research also assumes that the instantaneous peak load observed in the upper neck, specifically the occipital condyles, is a significant predictor of tensile neck load as opposed to an approximated peak load duration.

Nature of the Study

Following a similar approach as the research conducted by Zinck and Satava, this research seeks to further Parr's (2014) implementation of the MANIC and aid in the safe development of HMD and ejection system. Specifically, this research seeks to develop a transfer function between human and ATD tensile neck load responses due to -Gz accelerative inputs. This transfer function will then be used to generate a risk curve directly applicable to aerospace

accelerative testing with ATDs. The methods used to develop the transfer function and risk curve will be addressed and discussed in Chapter 3.

Summary

Evaluating existing data and developing a transfer function is the core of this research and will be expounded upon in Chapters 3, 4, and 5. Other research methods have been used to attempt to further ATD biofidelity and the usefulness of ATD data and are discussed in Chapter 2.

II. Literature Review

Introduction

The Air Force (AF) has equipped its modern fighter pilots with Helmet Mounted Displays (HMD) that enhance and increase the pilots' abilities to perform missions. However, increased HMD capabilities often increase helmet weight and shift the head's Center of Gravity (CG), which increase loads and moments on the pilots' necks (Buhrman, 1994). To minimize pilot injury and fatigue during the use of HMD, limits on HMD weight and CG location need to be developed. These limits should ideally be developed in part from an analysis of neck loads and moments experienced during ejections and accelerative tests.

Anthropometric Test Devices (ATDs) are the primary source of data used to evaluate ejection system safety and understand the likelihood of human neck injury in highly accelerative environments. However, the biomechanical differences between ATDs and humans have raised concerns that the results from ATD testing are inaccurate and either constraining the design space for HMDs and ejection systems by imposing overly harsh limits or are putting the pilots at unacceptable levels of risk of injury (Seemann, 1986; Herbst et al., 1998). Therefore, methods to compensate, such as a transfer function, are required to relate neck loads and moments measured by ATDs to equivalent neck loads and moments experienced by live humans.

The purpose of this research is specifically to enable a more robust application of a human based neck injury criteria that the United States Air Force adopted called the Multi-Axial Neck Injury Criteria (MANIC) more applicable to testing with ATDs. The Air Force Life Cycle Management Center (AFLCMC) has a requirement that aircraft escape systems do not induce more than a 5% risk of injury of a two or greater on the Abbreviated Injury Scale (AIS) for fully

equipped pilots (Parr et. al., 2015). The following graphic (Figure 1) provides a broad overview of how the ATD-to-human transfer function fits into the process of calculating a probability risk of neck injury from data collected in ejection tests as discussed earlier (Zinck, 2016; Satava, 2017).

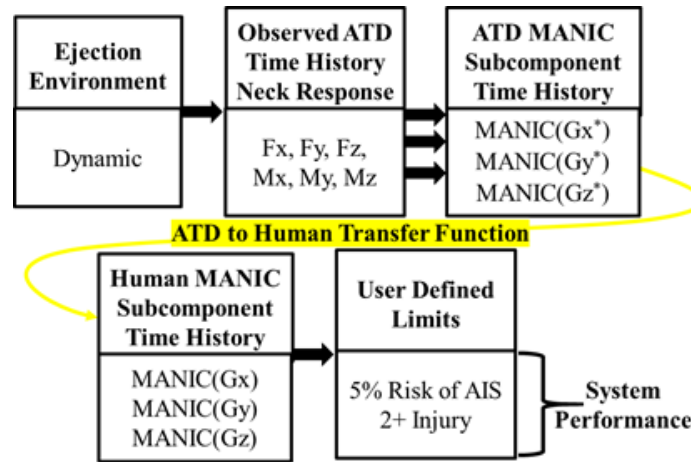


Figure 1. Overview of ATD to Human Transfer Function Implementation

The appropriate methods and assumptions to produce the transfer function will be explored through a literature review of previous work by Zinck (2016) and Satava (2017), other ATD tests from other fields such as the automotive safety industry, and statistical methods appropriate for the type of data collected from ejection and accelerative tests.

MANIC

The MANIC was created by Parr (2014) using a combination of low-accelerative, non-injurious tests of human volunteer subjects and high accelerative, often injurious, tests of and Post Mortem Human Subjects (PMHS). That novel combination allowed for the creation of probability risk curves that predict injury at various accelerations due to a combination of forces and moments on the neck. The MANIC provides quantitative neck injury criteria. Parr's work

improved upon previous neck injury criteria and provides the ability to quantify the risk of injury (Parr, 2014; Parr et al., 2013; Parr et al., 2014, Parr et al., 2015). Zinck provided additional insight into and overviews of the following important criterion: Nij, NIC, Beam, and Mertz tensile neck injury criteria (Zinck, 2016).

The MANIC is broken down into three elements (MANIC(Gx), MANIC(Gy), and MANIC(Gz)) and are shown in the table below. For each element of the criteria, there is an assigned numerical limit that corresponds to a 5% risk of AIS 3+ injury (Parr, 2014). In each axis, the MANIC’s elements are composed of the most important forces and moments on the neck where each of the terms is normalized by a critical value, detailed in Parr’s (2014) research. MIL-HDBK-516b details the United States Air Force’s (USAF) adoption of the MANIC and includes the critical values used in the individual elements.

Table 1. MANIC Summary (Parr, 2014)

Criteria Element	Limit
$MANIC(-Gx) = \left \frac{F_z}{F_{Zcrit}} \right + \left \frac{M_y}{M_{Ycrit}} \right $	Peak MANIC(-Gx) < 0.56 Less than 5% Risk of AIS 2+ Injury (<0.72 for AIS 3+)
$MANIC(Gy) = \sqrt{\left(\frac{F_x}{F_{Xcrit}}\right)^2 + \left(\frac{F_y}{F_{Ycrit}}\right)^2 + \left(\frac{F_z}{F_{Zcrit}}\right)^2 + \left(\frac{M_y}{M_{Ycrit}}\right)^2 + \left(\frac{M_z}{M_{Zcrit}}\right)^2}$	Peak MANIC(Gy) < 0.48 Less than 5% Risk of AIS 2+ Injury (<0.53 for AIS 3+)
$MANIC(-Gz) = +Fz$	Peak MANIC(-Gz) < 922 N/207 lb Less than 5% Risk of AIS 2+ Injury (<1136 N/256 lb for AIS 3+)

In Parr’s (2014) research, he noted that for the MANIC to be ready for implementation into a USAF qualification standard to evaluate the safety of an escape system or HMD in developmental testing using an ATD, it was likely that scaling would be required to accurately translate ATD neck loads into human neck loads, as ATDs are not perfectly biofidelic. The



relationship between the ATD and neck responses at varying accelerations provides essentially a scale factor to take ATD test results and translate them to the forces and moments a human would have experienced. Those human-equivalent loads are then plugged into the MANIC elements' equations to determine the probability risk of injury during that test event. That probability of risk informs the decision maker, for HMDs, ejection seats, and other equipment which might influence neck forces and moments on whether to pass the system. The MANIC has highlighted the United States Air Force's defined pass/fail criteria as shown above in Table 1 but has the ability to limit injury to any user-defined percentage at a defined injury risk level.

Figure 2 shows how laboratory tests are conducted on one axis and direction at a time and produce force and moment neck loads in response to accelerative level input. Those loads are plugged into the MANIC elements for each axis and the resulting MANIC values are compared to the human-based risk function. The escape system/HMD acquisitions decision maker then uses the resulting percent risk of injury to compare current or new designs to a numerical standard. That comparison to a standard can then be used to rank multiple competing designs against each other (Parr, 2014).

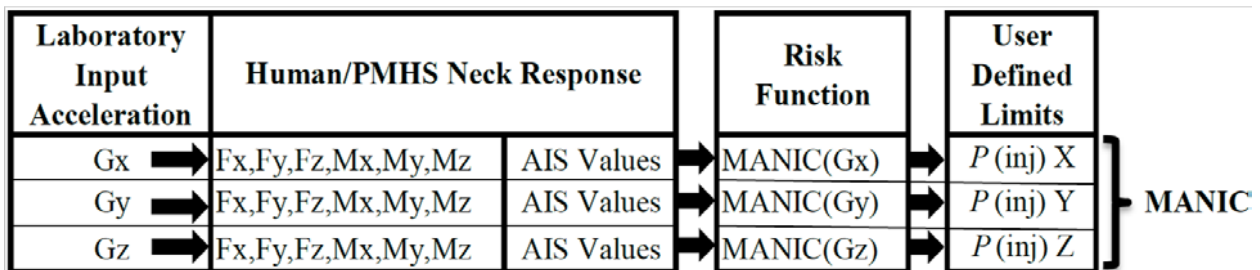


Figure 2. Overview of Development of the MANIC's Risk Functions

MIL-HDBK-516CN-5b

The military standard for ejection seat testing (MIL-HDBK-516CN-56) has incorporated Parr's (2014) human-centric risk functions and associated metrics, yet requires that all system level performance, as integrated into the aircraft, be verified by exposing instrumented ATDs to acceleration levels and collecting neck loads experienced during ejection. The following table shows the three axial components of the MANIC.

Table 2. X, Y, and Z Axial Components of the MANIC

Acceleration Axis	Definition
MANIC(-Gx)	$\left \frac{F_z}{F_{zcrit}} \right + \left \frac{M_y}{M_{ycrit}} \right $
MANIC(Gy)	$\sqrt{\left(\frac{F_x}{F_{xcrit}} \right)^2 + \left(\frac{F_y}{F_{ycrit}} \right)^2 + \left(\frac{F_z}{F_{zcrit}} \right)^2 + \left(\frac{M_y}{M_{ycrit}} \right)^2 + \left(\frac{M_z}{M_{zcrit}} \right)^2}$
MANIC(-Gz)	$+F_z$

Ejection Events

Ejection events of USAF fighter pilots are not a common occurrence relative to many of the other potentially deadly operations the USAF conducts. Looking at a slice of the data, for USAF F-16 pilots, 175 ejections have occurred since 1978 (36 in the 80s, 95 in the 90s, 44 in the 00s) which averages to only 4.5 per year (Bennett, 2009). However, ejection events and fighter pilots are integral to the public reputation of the USAF. As the USAF has both incorporated heavier HMDs and widened its parameters for pilots for pilot weight and height (103-245 pounds and 64-77 inches), the injury rate during ejection events is projected to surpass previously accepted standards (APP Business Plan, 2017). Most ejection events attain some level of fame simply because of their sensational videos and undergo additional levels of public scrutiny when

incidents involve the loss of aircrew lives. Therefore, if ejection events are not mandated to remain relatively survivable events, then the public's perception of the military would drop, and pilot's anxiety levels would rise. A doctoral dissertation followed by multiple master's theses seems like a lot of work to dedicate to an event that happens so rarely, but fighter pilots are oftentimes the USAF's public image. Pilots should not have to give up their confidence in their last effort escape route and start to anxiously think that ejecting is just as sure a means to death as crashing. The Aerospace Physiology and Performance (APP) program was established partly to address this critical aircrew safety issue and will continue to conduct research, experimentation, verification, and validation operations through the year 2024 (APP Business Plan, 2017).

Ejection events usually occur in six distinct stages and have unique types of acceleration during each stage. An ejection event starts with the highest acceleration level as the occupant (and seat) is ejected upward, clear of the aircraft, and their spine and neck are compressed. Next, the occupant is further propelled upward to a safe altitude, at a lower acceleration, by the seat itself. As the occupant is being propelled upward, and as soon as they clear the aircraft, windblast produces a frontal impact as the occupant slows down, yielding an acceleration similar to a car crashing into a wall. During this stage, the occupant's arms, legs, and head can flail about due to wind buffeting. Soon after, the drogue chute is deployed from the rear of the seat and produces another large acceleration in the $-X$ direction. This again accelerates the occupant forward and whips their head (and helmet) forward. Second to last is the vertical acceleration produced during the main parachute opening. The main parachute deploys above the occupant, the ejection seat detaches from the occupant, and the parachute opens by catching air. The parachute is attached to the pilot's torso, so the parachute opening shock pulls the pilot's torso

toward their head and causes compression and flexion of the neck. Additionally, the occupant's head may bend or flex to the side depending on the orientation of their head prior to the parachute opening. Lastly, the parachute landing fall is a maneuver executed by the occupant where they land and roll to disperse their momentum across their body. If the occupant has a severe neck injury from one of the previous stages, this stage is much more complicated and dangerous.

During all the ejection event's phases, a couple of key factors can increase the risk of neck injury for pilots. Proper alignment of the pilot's head and of the ejection seat itself (with reference to being completely upright) are important for keeping the probability of injury low. The ejection seat can wobble in midair because of uneven air drag due to misalignment of the pilot's head, arms, or legs. Wobble can also result from the small air bags that the Joint Strike Fighter's ejection seat deploys to keep the pilot's head as stationary as possible; specially to reduce neck flexion due to a heavy HMD (Seligman, 2015).

In any of these cases, a pilot's head or seat that is out of position can cause asymmetric forces and moments on the neck during the accelerations of each phase. From the moment that the pilot yanks on the ejection handle, if their neck, body, or appendages are out of alignment, even such a simple scenario as if they were looking down at the handle as they pulled it, that produces a drastically higher set of forces and moments than if their head were facing forward, directly stacked over the spine for support. Starting an ejection event out of alignment causes the pilot to begin each successive phase continually out of alignment with no hope of correction. The misalignment propagates as the phases are interconnected and far too dynamic to allow for the pilot to course correct.

Additionally, differences in body weights and gender can greatly affect the forces and moments experienced. Previous studies have shown that females experience greater neck loads than males at the same accelerative levels (Perry, 1998). This is because of their smaller cross-sectional area of the spine in the neck and a lower bone mineral density in the same area (Gallagher, 2007). Lightweight people have also been shown to experience greater forces and moments in their neck than middleweight or heavyweight people due to their smaller amount of tissue and muscle available to absorb the accelerative loads in their neck.

Anatomical Axes and Points of Reference

This study will use the same anatomical axes and neck load references as described by Satava (2017). It should be noted that the acceleration directions are in reference to the body (Figure 4) and the neck and head experience complex, multi-axial responses to the combined loading experienced during ejection events. The forces and moments experienced by the neck can vary between ejection events due to differences between occupants and starting positions of their bodies and heads.

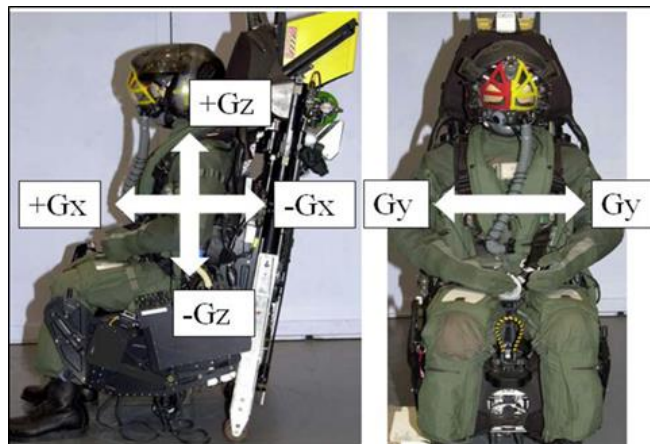


Figure 3. Acceleration Axes (Parr, 2014)

AIS 2 and 3 – Injury Classification

The AIS is an internationally recognized anatomical scoring system maintained by the Association for the Advancement of Automotive Medicine (AAM) (AAM, 2017). Injuries are classified on a point-scale, shown in Table 1, to identify the associated threat to life of an injury. MIL-HDBK-516C, specifies that applied and inertial forces during escape does not induce more than a 5% probability of AIS 2 or greater injury severity level as defined below throughout the required performance envelope.

The AIS was developed by what is now the Association for the Advancement of Automotive Medicine to fill the need for a standardized system for classifying type and severity of injuries resulting from vehicular crashes. The AIS was adopted as the standard for crash investigation teams funded by the US Department of Transportation as well as many academic and industry research organizations in the US and internationally. It therefore provides a widely accepted standard of injury classification with which to correlate with injury probabilities. Congress has mandated a 5% risk of AIS 2 injuries as their accepted limit for the neck during ejection. That is important because ejecting and becoming unconscious because of an injury or having a more than moderate injury is a worse scenario for a pilot who could be over water, enemy territory, or rough terrain and still must complete their landing by parachute. Contrast that with a neck injury for the driver of a car who is injured during an accident, the driver does not necessarily need to stay conscious after an accident especially as an ambulance may be on the way soon and they are not in enemy territory.

Lack of Data

There is not sufficient justification for loading up fighter pilots with additional sensors (with the sole function of recording ejection event data) that would have to be calibrated regularly and checked along with the many other pieces of equipment during a preflight check. The current method to estimate the force on a human neck during accelerations is to equip the subject with an accelerometer that they hold in their mouth (see Figure 6 below) and then use the weight of the subject's head, the circumference of their neck, and the distance from the accelerometer to their occipital condyles (the parts of the skull that form the neck joint with the uppermost vertebrae, enabling the head to move relative to the neck) to calculate force and moment estimates. The sensors would encumber the pilot and distract them from their primary duties and useful data would only be collected from the sorties in which ejection occurs. So, the best ejection event representative data we can collect is from animals, PMHS, and ATDs.

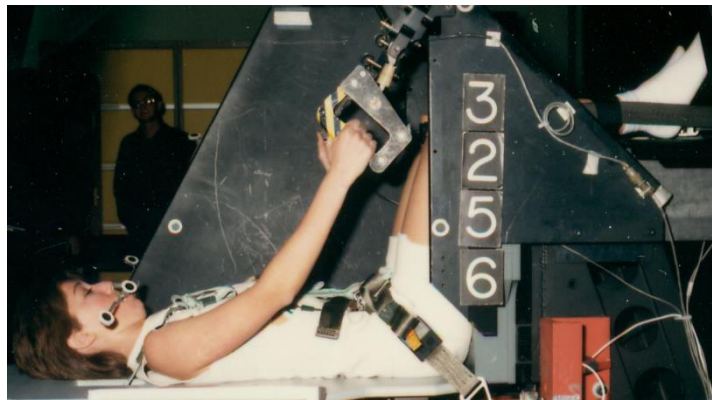


Figure 4. Laboratory Acceleration Test Subject Equipped with Bite-bar Accelerometer

ATDs and PMHSs are surrogates to evaluate neck loads in acceleration environments that are potentially injurious to humans. However, the internal reactions of human musculature, tendons and joints are difficult to emulate via ATD and PMHS experiments. Results from human volunteer testing with the same subject and input conditions have been known to be

highly variable. Continued research in ejection kinematics is required to build a more accurate surrogate for ejection testing (Salzar et al., 2009).

To date, computer models and physical models are insufficient for studying ejection event neck injuries. Many researchers (Bredbenner et. al., 2013) are looking into modeling the human neck. Unfortunately, no existing model is robust under the combination of accelerations experienced during an ejection. There are computer neck models that are useful for neck injury for workplace ergonomics, but they do not yet accurately predict human neck response at high accelerations (Spittle et al., 2009). Using automotive test data, NASCAR data, or commercial airline crash data do not provide applicable measurements due to dramatically different conditions. This section explained why the most obvious sources of data cannot be used, and the following sections will explain where all the data originates, and the different types of tests conducted to collect all the data. Each of the test and subject types are used together to build an approximation of all the accelerative levels, forces, moments, and injuries experienced by a live human during a full-up ejection event, an event which can never be fully observed.

Rocket Sled Tests

Rocket sled tests are where the cockpit and nose of an aircraft are attached to a rocket sled and an ATD is correctly harnessed to an ejection seat within the cockpit. The partial aircraft is accelerated down the length of the track until it reaches the desired speed and then the ejection system is activated. The ATD experiences the dynamic combined accelerations produced during a full ejection event and the internal neck forces and moments are recorded throughout.

Laboratory Tests

Laboratory tests are performed by focusing on one axis and one direction along that axis. These types of tests are currently conducted at the AFRL Human Performance Lab at Wright-Patterson AFB, OH. The two main test facilities used for this testing are the Horizontal Impulse Accelerator (HIA), and the Vertical Deceleration Tower (VDT). The VDT is used only for acceleration in the upward vertical direction. This is done by seating humans or ATDs in a vertical seated orientation then dropping them onto a pool of water which rapidly decelerates them. They are dropped a certain distance that corresponds to the desired accelerative load. These tests replicate single phases of ejection events such as the initial ejection acceleration, secondary acceleration, and parachute opening.

The HIA operates by delivering an accurate impulse to the subject and ejection seat with a gas-driven piston to induce a desired acceleration load for a certain impulse length. The subject and sled are free to travel the length of a 100m track as they gradually coast to a stop. The HIA can be used for each axis and direction of acceleration by orienting subjects in an ejection seat that is lying down, upright, or upright while side-facing relative to the sled track. These orientations provide acceleration along the X, Y, or Z axis to achieve single axis, single direction acceleration tests. The seat can be oriented in both directions along each of the three axes by configuring the ejection seat appropriately. These tests are simplified versions of singular phases of an ejection sequence and are important for breaking down the highly complex, wildly dynamic ejection event.

Human volunteers are only allowed to participate in laboratory tests if the test is at an adequately low accelerative level. During the tests, the subjects can be used to test any combination of the many designs of HMDs, seat harnesses, or ejection seats. Additionally, the

subjects can be instructed to brace for impact to varying degrees. The test conductor will also vary other parameters such as impulse duration, peak acceleration, and subject anthropometry.

ATD Testing

ATD testing is necessary because of the inherent risk to humans in testing at high accelerative levels. The USAF does not allow human test subjects to be exposed to forces which have the potential to cause irreparable even minor injuries. Also, ATD testing is necessary because of the cost and difficulty inherent in using PMHSs. Both ATDs and PMHs lack live musculature and thus cannot brace in the same way that humans can and usually do during ejection events.

The drawbacks of ATD testing arise because of the complexity of the human neck (Chancey et al., 2007). The neck has not been successfully modeled to a degree of fidelity to predict the outcome from high accelerative level testing (Bredbenner, et al, 2013). Thus, it follows that an ATD cannot be designed to mimic the human neck. From a visual standpoint, humans and ATDs have very different spinal structures (Figure 5).

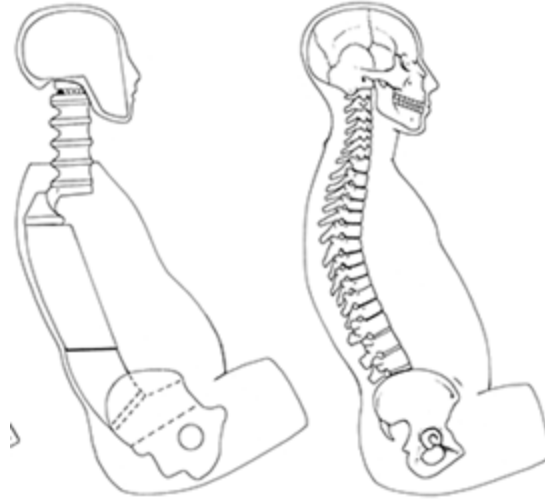


Figure 5. Side-by-side Comparison of ATD and Human Spinal Structures

There have been efforts by the Navy Research Lab to make ATDs have similar neck responses to humans by tweaking various material properties and tensioners in their neck piece parts, but the results were only partially successful (Seemann, Muzzy, and Lustick, 1986). Satava's (2017) research presents recent examples of visual and measured response differences between ATD (specifically average sized ATDs with the Hybrid III neck) and human necks in similar test events.

PMHS Testing

PMHSs are useful in each type of test for determining how specifically a human could be injured at various accelerative levels. In one test, PMHSs' spines were affixed to a stationary test apparatus and the head was then pulled at a specified loading rate to induce a purely tensile force (Specker and Plaga, 1996). The tensile loading rates were within a range of rates measured in manikins during ejections tests performed by the Air Force Research Laboratory (AFRL) (Specker and Plaga, 1996). Those ejections tests were conducted with SKIF (a Russian type

manikin) and Advanced Dynamic Anthropomorphic Manikin (ADAM) type manikins in the Russian K-36D ejection seat (Specker and Plaga, 1996).

After the tensile loading test, the PMHSs were autopsied to determine the presence of injuries and their severity. These injuries, and the associated tensile neck load that they occurred at, are used in developing risk curves. Tensile neck loads collected during PMHS testing at varying high accelerative levels provide the data needed to predict injury at the upper end of the operational accelerative envelope.

Fuller Envelope – New Air Force Body Types Accepted

The USAF recently allowed pilots with a wider range of heights and weights (APP Business Plan, 2017). While that is great for improving the pool of pilot applicants, this complicates the normalizing of risk calculations and likely constrains the number of potential equipment configurations which do not provide greater than allowable risk for at least some individuals within certain weight, gender, and height categories. Parr (2014) summarized previous studies where it was shown that a spinal difference in bone mineral density between males and females exists and that difference was a significant physical factor in explaining the large difference in neck loads experienced by males and females at the same accelerative loads. Additionally, smaller pilots are required to support a proportionally higher HMD mass when compared with their overall body mass.

The greater internal neck forces that females and lighter weight people experience put them at a higher probability of injury than males and heavier weight people because of their smaller neck bone structures and supporting musculature (Buhrman and Wilson, 2003; Perry, 1998). This increased risk, compounded by the requirement to evacuate the heavy, mandatory

HMD from the aircraft within a permissible time window, has grounded a large portion of the JSF F-35 pilot community until a solution can be found. Seligman (2015) broke the news on the increased risk of neck injury to lighter weight pilots of the F-35 Joint Strike Fighter (JSF), especially those weighing less than 136 pounds.

Transfer Function

Parr (2014) asserted that follow-on work should be undertaken to produce a mathematical relationship between ATD and human/PMHS accelerative test data to make the MANIC directly applicable to ATD testing. His neck injury criteria, the MANIC, should be used as the response variable as it is human/PMHS specific as well as specific to each of the three axes. ATD data from ejection event tests can not be directly used to predict human neck responses because of the significant biofidelic differences and the lack of injury data. The ATD data are either lower and thus constraining the design of ejection systems or are higher and are putting pilots at additional neck injury risk. A transfer function would compare the relationship between accelerative load and MANIC response (in each axis) for human and ATD necks.

Research by Zinck (2016) and Satava (2017) investigated transfer function development for the X and Y axes of acceleration. This research will focus on the z-axis transfer function (which focuses on neck tensile forces) for two reasons: neck tension has been found to be a significant predictor of neck injury (FAA, 2017), and for the z-axis of acceleration, tensile load was the only common neck load between available human subject and PMHS data sets during the creation of the MANIC (Parr, 2014).

The difference between ATD and human neck response is significant enough to warrant the work needed to create transfer functions. For example, Satava (2017) showed a significant

difference in the following pictorial comparison in Figure 7. The figure is from a side-facing sled test to measure neck loads in response to Y-axis accelerations and shows a human and ATD during identical test runs. The top row of images shows the human's neck response to the acceleration is a combination of twisting, flexing, and bending. However, the ATD's response to the same acceleration is almost entirely bending.

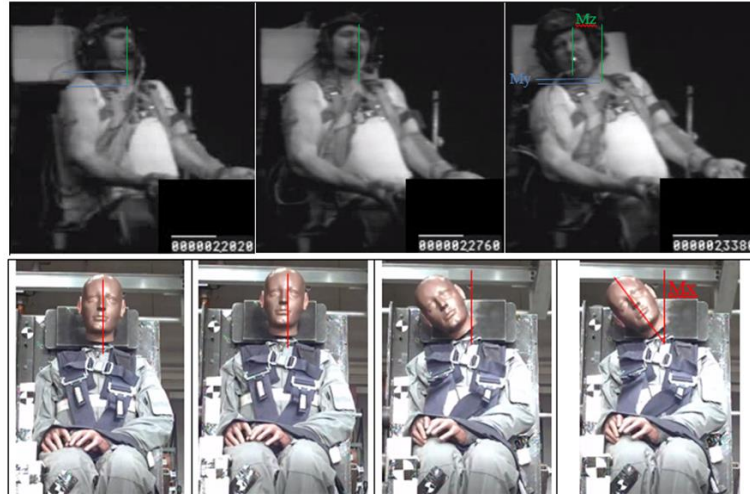


Figure 6. Difference in Head/Neck Response to Similar GY Accelerative Input (Satava, 2017)

The differences in Figure 7 were not only visible but also measurable in a single-axis, single-direction laboratory test, and thus the differences at full ejection event accelerations would necessarily be greater. The differences support justification of a transfer function being created for the third axis of the MANIC.

The transfer functions are important because when the ATD and human neck responses are significantly different, then there are significant consequences to using ATD data as if it were from a human. For example, if the ATD data are consistently higher than the human data, then the HMD and ejection seat designs are constrained by the inaccurately high ATD neck load

responses. Contrarily, if the ATD data are consistently lower, then the inaccurately low ATD neck load responses are putting the pilots at an unintentionally high risk of neck injury.

Because ATDs do have significant biomechanical differences from humans, the use of ATDs as proxies for humans in ejection event tests may be doing more harm than good as there are HMD and ejection seat designs passing the MANIC based solely on ATD test data. Once transfer functions for all three axes are created, the benefits of using ATDs would be more fully realized. The benefits would be either expanding the envelope for HMD ejection seat designs or decreasing the actual risk of neck injury for pilots by failing those designs that fall outside the parameters for the MANIC.

Risk Curve for ATDs

Once a transfer function is developed for the z-axis, the human-data based probability of injury risk curve in the MANIC(Gz) can be converted to an ATD probability of injury risk curve. This risk curve would be created by converting the human and PMHS data (that was used to create the original MANIC(Gz)) to equivalent ATD data while keeping the same injured/non-injured status after the conversion, and then producing a cumulative distribution function that best represents the converted data. The risk curve would be important for ejection event tests that are conducted without the ability, or with the failure to, collect accelerative loads during the test sequence. The only data needed from such an ejection test would be the internal forces and moments recorded within the ATD's upper neck. That ATD neck load data would be used on the ATD risk curve to calculate the corresponding probability of neck injury risk for a human.

III. Methodology

Introduction

This chapter describes the methods used to develop an ATD to human tensile neck load transfer function and an ATD tensile load neck injury risk curve. Linear regression through the origin will be used to construct a model relating acceleration and tensile neck load response for both humans/PMHS and ATDs. The best model will be selected to most accurately reflect tensile neck load differences between ATDs and humans at varying Gz accelerative inputs. A transfer function will then be defined using the proportional difference in tensile neck load responses between the ATD and human models. Lastly, an ATD tensile neck injury risk curve will be developed by applying survival analysis to ATD tensile neck loads generated from the transfer function after converting human/PMHS tensile neck loads along with their associated injuries to equivalent ATD tensile neck loads.

Transfer functions for two of the three axes of acceleration have been developed using linear regression and multiple regression. The development of an appropriate transfer function for the remaining axis (the vertical, z-axis) is the primary focus of this research, but the previous research's analytic techniques will also be used to provide direct comparison to past results.

Original Data Source

Test data used for this analysis was collected from the existing literature and the USAF Biodynamics databank (BIODYN), a part of the Collaborative Biomechanics Data Network (CBDN) that is operated and maintained by the Human Effectiveness Directorate (RH) under the 711th Human Performance Wing at Wright-Patterson AFB, OH. All corresponding tests were conducted on the Horizontal Impulse Accelerator (HIA) located at Wright-Patterson AFB, OH.

The BIODYN on the CBDN served as one of the primary data sources for this research. The BIODYN data naming convention is by year and calendar test number iteration, e.g. the 10th study conducted in 2016 is annotated as '201610'. The naming convention for each test run within a study is by facility and iteration number, e.g. HIA test 6557 is annotated as HIA6557. To create human Gz risk functions, Parr (2014) used human Gz test results from the BIODYN 198504 study and combined PMHS injury data from three separate studies.

For the Gz axis of acceleration, tensile load (+Fz) was the only common neck load available between human subject and PMHS data, thus a tensile only neck injury risk function resulted, which will be referred to as MANIC(-Gz) (Parr, 2014). The live human subject experimental neck load data used to construct the risk function came from previous AFRL tests where the subject was seated in a test ejection seat, but oriented horizontally (Brinkley and Getschow, 1988). An impulse of acceleration was applied to the seat such that the subject's body was accelerated away from their head, resulting in a neck response that was observed to be primarily tensile loading of the cervical spine. The data from that study will be used in this research is in Chapter 4. No new data from human subject experiments in this orientation have been published since, therefore this data remains the best source of live human subject neck tension data. This research will use the human subject and PMHS data from Parr (2014) to comprise the human relationship between -Gz accelerative load and the resulting tensile neck load response. Parr (2014) supplemented the small number of PMHS data points from Z-axis tests using PMHS data from Cheng's research (1982) in -Gx frontal impact tests. It is assumed that -Gx accelerative loads do not have the same correlation to tensile neck load as -Gz accelerative loads. Therefore, a separate transfer function will be developed to convert the -Gx

PMHS data points to equivalent ATD data points. This will be done in the same manner as the -Gz transfer function.

The second data set used in this research is from two studies of tensile neck load forces measured from Hybrid III 50th percentile male Automotive ATDs. The studies were chosen because they are the only available accelerative studies in the -Gz direction that capture both accelerative level and internal upper neck tensile load.

To determine human tensile neck loads (at the occipital condyles) from the data taken from BIODYN, angular accelerations measured on a bite-bar accelerometer were converted to neck loads using each subject's anthropometric factors (e.g. head circumference, neck size, etc.) using the Neckload4 program. This is the same program used by Parr (2014) and Parr et. al. (2015), which was created by AFRL to make these specific conversions and maintain results comparability. Additional details about Neckload4 functionality and assumptions are presented in Appendix C in Satava (2016).

Once the data sets were chosen, each study was screened for anomalous data. Responses of the six primary neck loads and moments (F_x , F_y , F_z , M_x , M_y , and M_z) and the sled accelerations (G_x , G_y , G_z) were plotted to ensure a nominal response during each test run. No test runs required censoring or removal from the data set. The peak tensile neck load and z-axis accelerative level were taken as the defining values for each test run as they were the only relevant values for this research.

Assigning Accelerative Loads to PMHS Data Points

It was necessary to assign accelerative loads to the -Gz PMHS data points to aid in forming the transfer function. The transfer function is a relationship between upper neck tension and accelerative load in the -Gz direction. The Yliniemi et. al. study (2009) did not directly associate an accelerative load to the PMHS tensile tests they performed. To associate an accelerative load to the PMHS data points, a methodology was developed to determine whether an approximate accelerative load could be calculated or found in a reference.

Linear Regression

Linear regression will be used to identify the relationship between the dependent variable, tensile neck load, and the input, accelerative load. Simple linear regression will be used to maintain comparability to previous research conducted by Zinck (2016) and Satava (2017), but also to aid in developing statistically significant models of human and ATD tensile neck load responses. There is not a need to perform multiple regression in this research as it was in Satava (2017) because the data comes from homogenous data sources. All linear regression models will be plotted using Microsoft Excel (2017) and validated using R.

Since it is intuitive that there should be a negligible neck injury risk and negligible neck loads at 0G, regression through the origin (RTO) was used by Zinck (2015) and Satava (2016) to develop MANIC(-Gx) and MANIC(Gy) regression models that met this assumption. RTO forces the regression model to have an intercept at zero which signifies a zero value of tensile neck load and a corresponding zero probability of injury if head accelerations are maintained at zero G. The same method will be used for tensile neck load responses.

Transfer Function

In this thesis, the term “transfer function” is used to describe the use of the relationship between the human and ATD regression models as a scaling factor to convert between subject types. The proportional difference in human and ATD tensile neck load values at a particular Gz acceleration is used to define the applicable transform between the two subject types. This application is not consistent with the method employed by Zinck (2015) and Satava (2016) for the development of a MANIC(-Gx) and MANIC(Gy) human to ATD transfer functions.

The previously used subtractive method by Zinck (2016) and Satava (2017) in the application of their transfer functions does not proportionally scale the responses from the human to ATD linear models and can lead to some tensile values being subtractively scaled to negative values, which is invalid. A scale factor method (through multiplication) solves both of those problems and adds the benefit of allowing the scaling of any live human or PMHS tensile data points regardless of whether they have an associated accelerative level. This is because both relationships are linear models with a (0,0) intercept and thus are at a constant proportional difference across all accelerative levels.

Survival Analysis

Currently, the human risk curves developed by Parr et al. (2014) are the Air Force standard for evaluating ejection system injury risk, per MIL-HDBK-516. However, the transfer functions for each axis of acceleration will be used to account for the biomechanical differences between humans and ATDs as ATDs are the subjects used in ejection tests. The MANIC(Gy) transfer function was used by Satava (2017) to convert the human and PMHS data points that were used

in Parr's (2014) risk curve to equivalent ATD data points. The injury/non-injury status of each human and PMHS data point was associated with the equivalent converted ATD data point. Survival analysis was then used to evaluate the probability of injury for ATDs at a given MANIC(Gy) value. This research will construct an ATD tensile neck injury risk curve in the same manner.

As explained in Parr (2014), non-injurious data points are considered right-censored and injurious data points are considered left-censored. For a more detailed explanation of censored data and its applicability to human injury data, refer to Parr (2014). The ATD risk curve will be constructed using parametric survival analysis in R (2017) which uses a maximum likelihood estimate to determine what form of an assumed distribution would best fit the data. Satava (2016) assumed the logistic distribution for the parametric survival analysis as logistic analysis has often been used to characterize probability of injury (Montgomery et al., 2006:429, Parr et al. 2015; Bass et al., 2006). All survival analysis will be accomplished with the Statistical Methods for Reliability Data package (2015) in R, RStudio: Integrated Development for R (2016) and R: A language and environment for statistical computing (2017).

IV. Results

Overview

The results in this chapter build up to developing the ATD equivalent AIS2+ and AIS 3+ risk functions by first starting with the -Gz PMHS data points that could be associated with an accelerative load and then the -Gx PMHS data points being converted to equivalent ATD data points through a -Gx transfer function. After those results, the rest of the chapter is focused on presenting the -Gz transfer function and tensile neck load risk curves. In each section, some sensitivity analyses are performed to determine the effect of changing certain assumptions.

Assigning Accelerative Levels to PMHS Data Points

The Yliniemi et. al. study (2009) stated that the test methodology was based on the Specker and Plaga (1996) study where AFRL conducted in-flight ATD ejection tests and measured neck loading rates during the windblast and parachute opening stages. Yliniemi et. al. (2009) referenced only one loading rate from a data point in the Specker and Plaga (1996) study, one that was conducted at 694 knots equivalent air speed (KEAS) and resulted in a loading rate of approximately 35 kN/s. Specker and Plaga (2009) then conducted calibration runs of their planned tensile loading test on ATDs to tune their actuator's displacement rate to the planned loading rate of 35 kN/s. The actuator displacement rates ranged from 520-740 mm/s and resulted in loading rates of 35-60 kN/s in the ATD's neck. Three of the PMHS test runs were conducted at an actuator displacement rate of 730 mm/s and the remaining nine were at 520 mm/s.

In the Specker and Plaga study (1996), the test parameters (pg. 41), ejection sequence timing (pg. 42), and seat accelerations (pp. 316, 320, 324, and 328) were compiled and are shown in the tables below.

Table 3. Test Number 11, 694 KEAS, Test Parameters. (Specker and Plaga, 1996)

Test No	Test Date	Designation	Manikin	KEAS	Airspeed (ft/s)	Mach	Altitude (ft)
11	9/16/1993	SL1295	ADAM (L)	694	1171	1.08	656

Table 4. Test Number 11, 694 KEAS, Ejection Sequence Timing (Specker and Plaga, 1996)

Seat 1st Motion, sec	Boom Firing, sec	Seat/Rail Separation, sec	Main Parachute Deployment, sec	Manikin/Seat Separation, sec
5.418	5.508	5.555	6.98	6.982

Table 5. Test Number 11, 694 KEAS, Seat Accelerations. (Specker and Plaga, 1996)

Max Seat Accelerations, G				
Accelerometer A	Accelerometer B	Accelerometer C	Accelerometer D	Average Value, G
24.5	24	26	25	24.875

The four seat accelerometers were attached to the seat in the test and were configured as shown in the figure below.

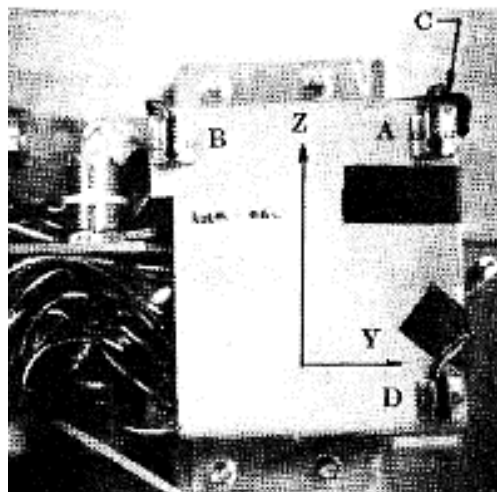


Figure 7. Seat Accelerometers on Mounting Bracket, (Specker and Plaga, 1996)

Accelerative load was a z-axis impulse input to the seat that the ATD was in, so the windblast stage occurs with the seat accelerometer intact, but the parachute opening stage does not. Thus, the peak seat accelerations collected during the windblast stage will be used to associate accelerative loads to the tensile loading rates measured in the ATD neck. The peak seat z-axis acceleration points were extracted from the following figures and averaged together to equal 24.875G.

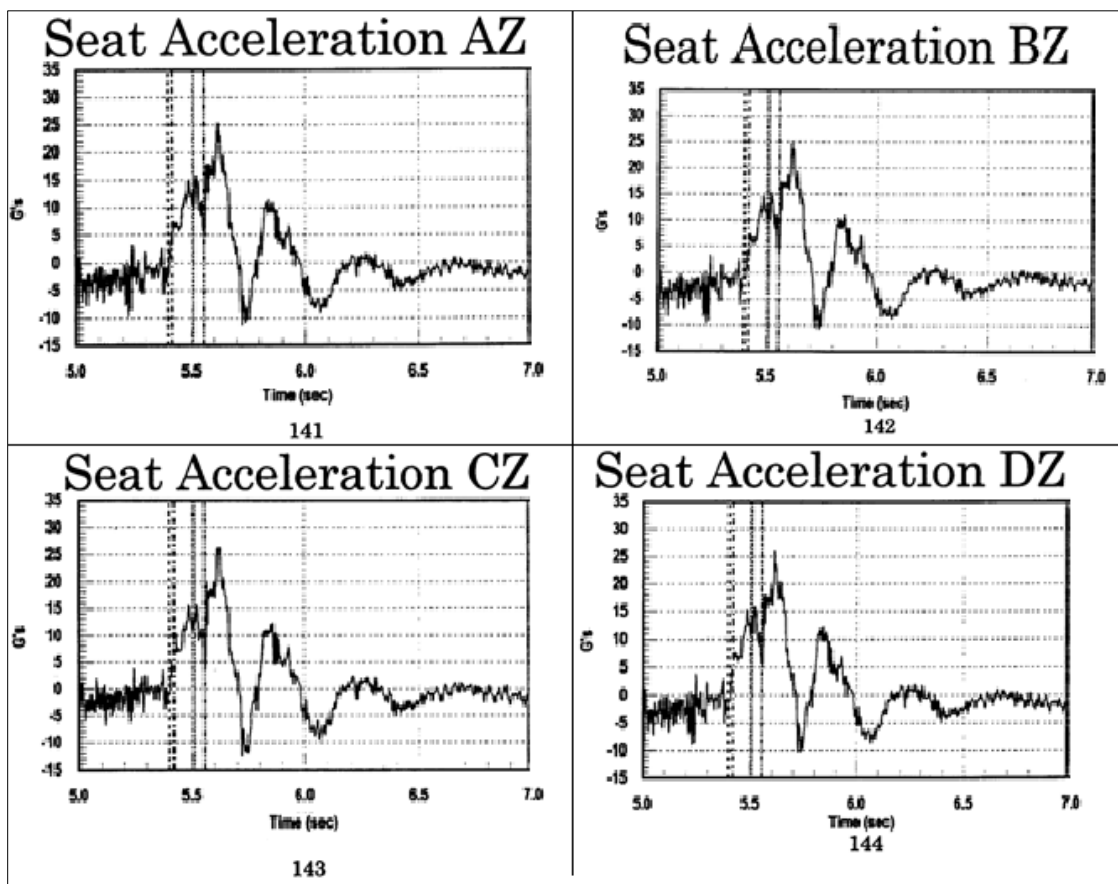


Figure 8. Test Number 11, 694 KEAS, Four Seat Accelerometer Data (Specker and Plaga, 1996)

The 2009 study is quoted as producing loading rates of 35-60kN/s when operating the actuator at displacement rates of 520-740mm/s. Thus, for the first three data points which were loaded at a rate of 730mm/s, the accelerative load of 34.921G was extrapolated from the two data points (0G at 0mm/s) and (24.875G at 520mm/s).

There was not any methodology or clues in the literature of the Yoganandan and Sances studies that allowed for an accelerative level to be associated with the tension values. Therefore, those PMHS data points will not be used in creating the transfer function but will later be converted to equivalent ATD data points using the transfer function.

-Gx Tensile Neck Load Transfer Function

As stated in Chapter 3, a -Gx tensile neck load transfer function is necessary to convert the -Gx PMHS data points, from the MANIC(-Gx) risk function, to equivalent ATD tensile neck loads. The assumption was made that the correlation between tensile neck load and each axis of acceleration is not identical. Therefore, the unique correlation of tensile neck load to accelerative load in the X-axis would require a separate tensile neck load transfer function from the rest of this research.

A linear transfer function between -Gx accelerative loads and upper neck tensile values was created by using the same live human and PMHS data points that Parr (2014) used in developing the MANIC(GX) risk curve and the ATD data points that Zinck (2016) used in creating his transfer function. The data are shown in the table below. The ATD data points were extracted directly from the BIODYN database. The transfer function, using the most likely estimates of the slope of the linear models, is shown in the Figure below. The data shows a

significant difference in how the necks of live humans and PMHS in -Gx acceleration produce tension values and how the necks of ATDs perform.

**Table 6. Human Data from -Gx Accelerative Studies
Used in Creating -Gx Transfer Function**

	Peak Accelerative Load, G	Tension, N	Censor	AIS 3+ Injury
1	8	152.7	R-censored	No
2	8	192	R-censored	No
3	8	230.3	R-censored	No
4	8	126.3	R-censored	No
5	8	111.2	R-censored	No
6	8	379.1	R-censored	No
7	8	103.5	R-censored	No
8	8	12.3	R-censored	No
9	8	221.8	R-censored	No
10	8	2.3	R-censored	No
11	8	170.4	R-censored	No
12	8	141.1	R-censored	No
13	8	18.4	R-censored	No
14	8	89.4	R-censored	No
15	8	430.6	R-censored	No
16	8	393	R-censored	No
17	8	129.5	R-censored	No
18	8	429.8	R-censored	No
19	8	3.8	R-censored	No
20	8	228.8	R-censored	No
21	8	0.1	R-censored	No
22	8	10.1	R-censored	No
23	8	182.7	R-censored	No
24	8	153	R-censored	No
25	8	321.6	R-censored	No
26	8	203.7	R-censored	No
27	8	240.1	R-censored	No
28	8	15.4	R-censored	No
29	8	470.7	R-censored	No
30	8	122.8	R-censored	No
31	8	183.6	R-censored	No
32	8	103	R-censored	No
33	8	7.9	R-censored	No
34	8	1.5	R-censored	No

35	8	77.6	R-censored	No
36	8	333.4	R-censored	No
37	8	202.1	R-censored	No
38	8	6.1	R-censored	No
39	8	238.3	R-censored	No
40	8	4.5	R-censored	No
41	8	3.2	R-censored	No
42	8	9.1	R-censored	No
43	8	449.4	R-censored	No
44	8	1.6	R-censored	No
45	8	72.4	R-censored	No
46	6	2.7	R-censored	No
47	6	115.2	R-censored	No
48	6	61.5	R-censored	No
49	6	41.9	R-censored	No
50	6	45.7	R-censored	No
51	6	188.4	R-censored	No
52	6	32	R-censored	No
53	6	12.6	R-censored	No
54	6	3	R-censored	No
55	6	3.3	R-censored	No
56	6	13	R-censored	No
57	6	38.2	R-censored	No
58	6	13.8	R-censored	No
59	6	4.8	R-censored	No
60	6	11.4	R-censored	No
61	6	23.9	R-censored	No
62	6	88.3	R-censored	No
63	6	7.1	R-censored	No

Table 7. PMHS Data from -Gx Accelerative Studies Used in Creating -Gx Transfer Function

	Peak Accelerative Load, G	Tension, N	Censor	AIS 3+ Injury
1	32	3490	L-censored	Yes
2	37	7200	L-censored	Yes
3	38	2420	L-censored	Yes
4	36	850	R-censored	No
5	37.5	6520	L-censored	Yes
6	39	3210	R-censored	No

Table 8. ATD Data from -Gx Accelerative Studies Used in Creating -Gx Transfer Function

	Study	Test Number	Subject Type	Peak Accelerative Load, G	Tension, N
1	199501	HIA5273	MANIKIN-M	10.17	85.08
2	199501	HIA5276	MANIKIN-M	10.1	89.16
3	199501	HIA5280	MANIKIN-F	10.16	116.18
4	199501	HIA5322	MANIKIN-M	10.06	179.49
5	199501	HIA5327	MANIKIN-F	9.72	121.85
6	199501	HIA5328	MANIKIN-F	21.64	643.03
7	199501	HIA5334	MANIKIN-F	20.76	637.29
8	199501	HIA5338	MANIKIN-M	20.1	421.69
9	199501	HIA5344	MANIKIN-M	30.71	1014.77
10	199501	HIA5346	MANIKIN-M	31.72	1014.34
11	199501	HIA5349	MANIKIN-F	30.31	1065.44
12	199501	HIA5350	MANIKIN-F	37.17	1046.36
13	199501	HIA5352	MANIKIN-F	35.93	1054.34
14	199501	HIA5354	MANIKIN-F	42.28	1051.76
15	199501	HIA5355	MANIKIN-F	44.76	765.53
16	199301	HIA4365	MANIKIN-M	5.58	1.46
17	199301	HIA4378	MANIKIN-M	7.05	2.67
18	199301	HIA4456	MANIKIN-M	8.51	13.37
19	199301	HIA4463	MANIKIN-M	9.68	25.53
20	199301	HIA4474	MANIKIN-M	9.88	27.05
21	199301	HIA4479	MANIKIN-M	8.46	11.11
22	199301	HIA4520	MANIKIN-M	8.53	24.75
23	199301	HIA4526	MANIKIN-M	8.58	28.25
24	199301	HIA4648	MANIKIN-M	8.59	21.88
25	199301	HIA4692	MANIKIN-M	8.47	24.69
26	199301	HIA4695	MANIKIN-M	8.48	38.58
27	199201	HIA4086	MANIKIN-M	9.76	63.87
28	199201	HIA4087	MANIKIN-M	9.87	77.53
29	199201	HIA4088	MANIKIN-M	9.94	78.89
30	199201	HIA4090	MANIKIN-M	9.86	83.46
31	199201	HIA4091	MANIKIN-M	9.87	84.41
32	199201	HIA4092	MANIKIN-M	21.18	371.29
33	199201	HIA4093	MANIKIN-M	21.23	437.21
34	199201	HIA4094	MANIKIN-M	21.18	544.1
35	199201	HIA4095	MANIKIN-M	37.6	1314.96
36	199201	HIA4096	MANIKIN-M	38.87	1329.6
37	199201	HIA4097	MANIKIN-M	37.85	1053.82

38	199201	HIA4098	MANIKIN-M	46.45	1743.8
39	199201	HIA4099	MANIKIN-M	46.4	1749.71
40	199201	HIA4100	MANIKIN-M	46.18	1752.02

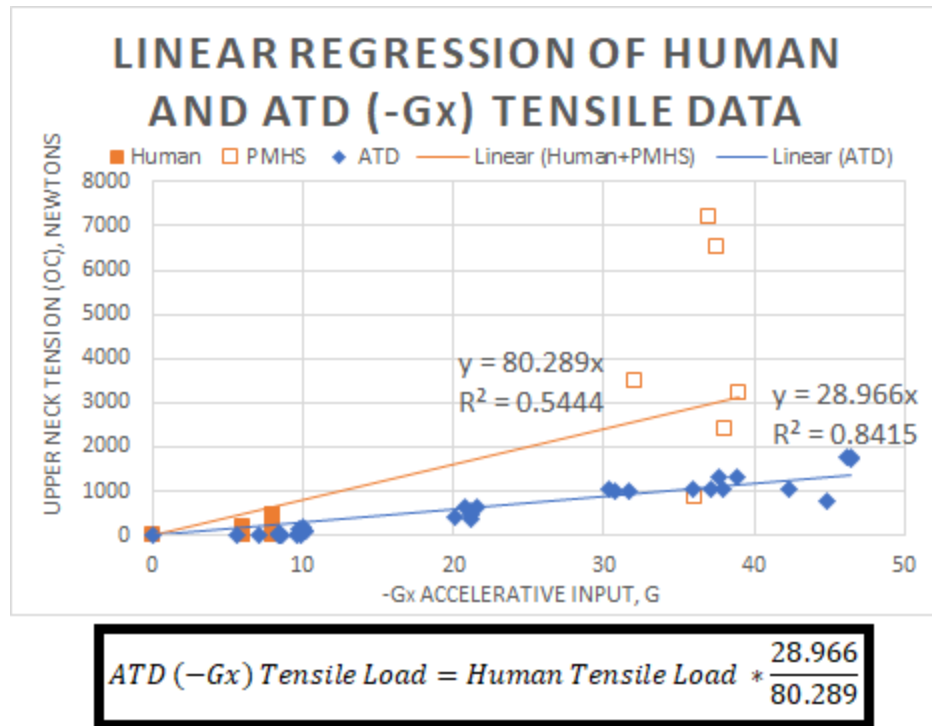


Figure 9. Linear Regression of Human and ATD (-Gx) Tensile Data and (-Gx) Transfer Function

The human and ATD linear models had p-values of less than 1.0E-10 which supports a linear relationship between accelerative input and tensile load. A test for constant variance for each data set resulted in p-values of less than 0.05 which does not support the assumption of a constant variance in the data. This non-constant variance violates one of the assumptions in linear models. However, none of the measured anthropometric or test parameters were able to explain the non-constant variance, so the linear model as shown was used.

Live humans and PMHS necks have a significant correlation between -Gx accelerative load and tension values that is close to the correlation between -Gz accelerative loads and tension

values. In his MANIC(-Gz) risk curve creation, Parr (2014) combined PMHS data points from -Gz and -Gx accelerative tests due to the need for more data points outweighing the fact that they are from studies in different accelerative directions. Therefore, the -Gx PMHS data points that Parr (2014) used will also be used in creating the ATD equivalent risk curve after converting them using a transfer function. However, the -Gx PMHS data points will be converted to equivalent ATD data points with a transfer function created from -Gx tests of live humans, PMHS, and ATDs. This is due to the difference in transfer functions between -Gx accelerative loads and tensile values and -Gz accelerative loads.

An important trend seen in the -Gx accelerative data is that there seems to be a higher correlation between accelerative load and tensile values for ATDs when the accelerative direction is -Gx rather than -Gz as it would naturally seem.

It is important to note the trend of live human and PMHS tensile force data points to have a higher variance at a given accelerative load as compared to ATD data points. The ATD data points have a smaller variance in tensile force response at a given accelerative load which seems to make sense as their anthropometric parameters are relatively constant as compared to the wide variation in live human and PMHS parameters. The trend of higher variance in tensile load for live human and PMHS data points and lower variance for ATD data points is consistent for both the -Gx and -Gz accelerative tests.

95% Confidence Intervals of Linear Models used in -Gx Transfer Functions

Next, a two-sided 95% confidence interval was calculated for the slope of each linear model to obtain a more and less conservative estimate for the relationship between accelerative level and tensile load. The 95% confidence interval for the slope of the linear model for

human -Gx accelerative tests is 80.29 ± 15.90 and the confidence interval for the ATD data is 28.97 ± 2.890 . The most likely estimate linear models, along with their respective 95% confidence interval estimates, are plotted in the figure below.

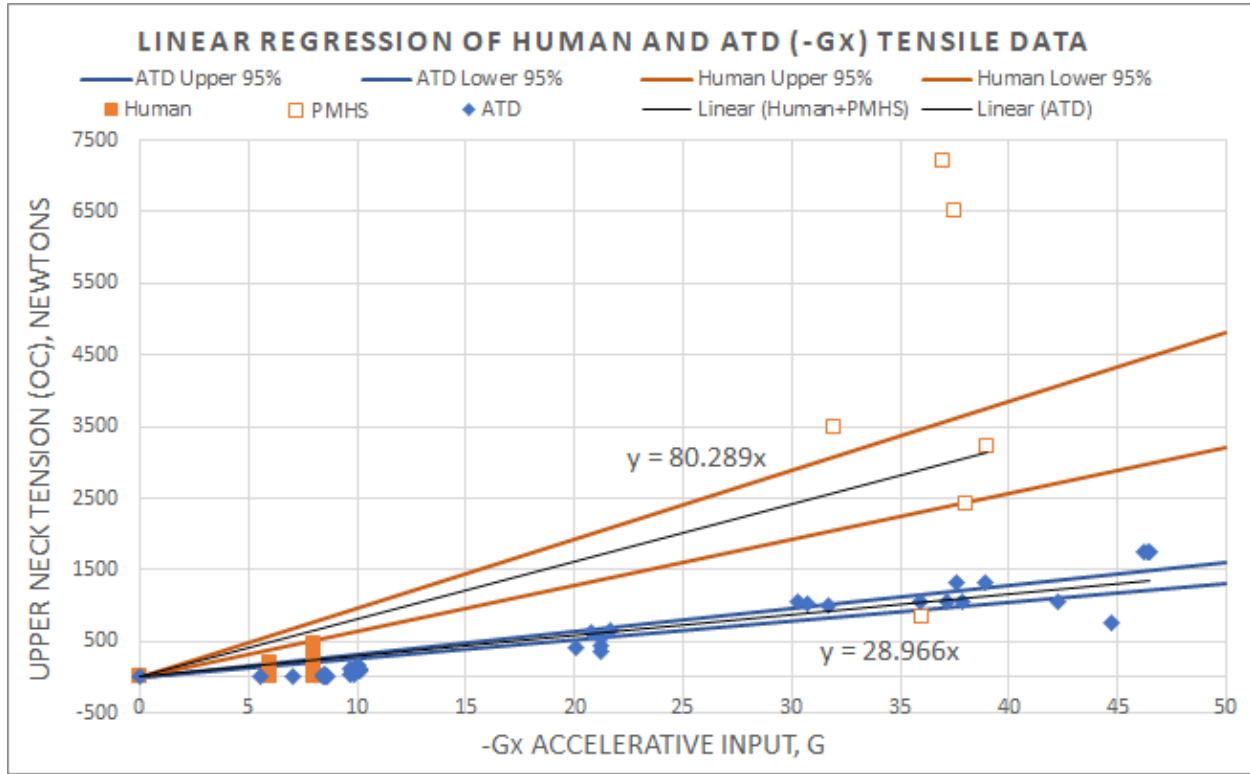


Figure 10. -Gx Tensile Neck Load Linear Regression Models and 95% Confidence Interval Bounds

Using the 95% confidence bounds for each linear model, the largest scale factor would result from using the human upper 95% bound and the ATD lower 95% bound. This scale factor would result in the largest difference in response between human and ATD tensile neck loads in -Gx accelerative tests. Converting between data types with such a transfer function would constitute a conservative approach to converting tensile neck loads from ATDs. The transfer function using this scale factor is shown in the figure below.

$$ATD (-Gx)Tensile Load = Human (-Gx)Tensile Load * 0.2711$$

Conversely, the smallest scale factor results from using the lower human 95% bound and the upper ATD 95% bound. This scale factor assumes a smaller difference between human and ATD neck loads in -Gx accelerative tests. Using this scale factor as the transfer function would constitute a less conservative approach to converting tensile neck loads from ATDs. The transfer function using this scale factor is shown in the figure below.

$$ATD (-Gx)Tensile Load = Human (-Gx) Tensile Load * 0.4947$$

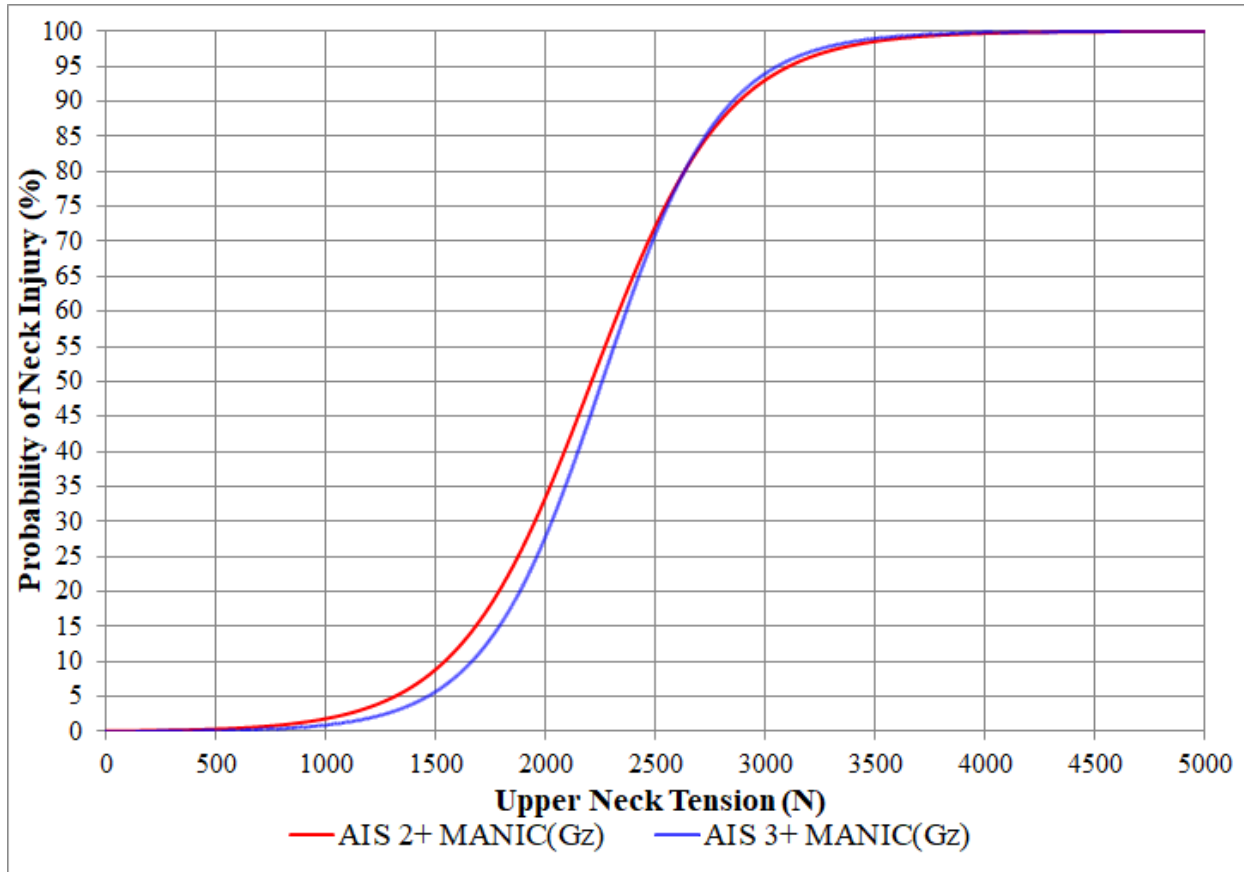
-Gz Tensile Neck Load Transfer Function

A linear transfer function between -Gz accelerative loads and upper neck tensile values was created by using the same live human and PMHS data points that Parr (2014) used in developing the MANIC(-Gz) risk curve. The live human data points are in Appendix A and the PMHS data are shown in the table below.

Table 9. PMHS Data from -Gz Accelerative Studies Used in Creating -Gz Tensile Neck Load Transfer Function

	Study	Approximate Peak Accelerative Load, G	Tension, N	Censor	AIS 3+ Injury
1	Yliniemi et. al., 2009	34.921	3560	L-censored	Yes
2	Yliniemi et. al., 2009	34.921	4060	L-censored	Yes
3	Yliniemi et. al., 2009	34.921	3860	L-censored	Yes
4	Yliniemi et. al., 2009	24.875	2250	L-censored	Yes
5	Yliniemi et. al., 2009	24.875	1910	L-censored	Yes
6	Yliniemi et. al., 2009	24.875	2810	L-censored	Yes
7	Yliniemi et. al., 2009	24.875	3150	L-censored	Yes
8	Yliniemi et. al., 2009	24.875	3230	L-censored	Yes
9	Yliniemi et. al., 2009	24.875	3220	L-censored	Yes
10	Yliniemi et. al., 2009	24.875	2440	L-censored	Yes
11	Yliniemi et. al., 2009	24.875	3230	L-censored	Yes
12	Yliniemi et. al., 2009	24.875	3490	L-censored	Yes

The live human data points were extracted directly from the BIODYN and run through the Neckload4 program to associate an accelerative load with each tensile load as Parr (2014) did not report that data as he did not have use for it. During the process, it was discovered that a mistake had been made in assigning the units to the tensile loads as the output from the Neckload4 program is pounds, but they were labeled as Newtons in Parr (2014). This is significant because each data point was off by the conversion factor between pounds and Newtons, which is a factor of 4.4458. The MANIC(-Gz) AIS 2+ risk curve was recalculated using all the tensile data points in Newtons, resulting in a 5th percentile value of 1313.0 Newtons (95% confidence interval (CI) 964.0 N, 1661.0 N), and is plotted in the figure below. The MANIC(-Gz) AIS 3+ risk curve was recalculated using all the tensile data points in Newtons, resulting in a 5th percentile value of 1462.0 Newtons (95% CI 1070.0 N, 1854.0 N), and is plotted in the figure below.



$$P(AIS \geq 2) = \frac{1}{1 + \exp \frac{2209.5 - Tension(Newtons)}{304.6}}$$

$$P(AIS \geq 3) = \frac{1}{1 + \exp \frac{2257.2 - Tension(Newtons)}{270.2}}$$

Figure 11. Corrected Human-based Risk Curves for Probability of Abbreviated Injury Scale (AIS) 2+ and 3+

The second half of the -Gz transfer function was created by using two studies of -Gz accelerative ATD tests available on the BIODYN database. The data are shown in the table below and were extracted directly from the BIODYN database. The -Gz transfer function is

shown in the figure below. The data shows a significant difference in how the necks of live humans and PMHS in -Gz acceleration produce tension values and how the necks of ATDs perform.

Table 10. ATD Data from -Gz Accelerative Studies Used in Creating -Gz Transfer Function

Study	Peak Accelerative Load, G	Tension, N	Direction and Axis	Test No	Manikin Type	
1	200803	18.77	461.490	-Z	HIA8144	HB3-50 Auto
2	200803	19.71	645.671	-Z	HIA8145	HB3-50 Auto
3	200803	19.24	428.935	-Z	HIA8146	HB3-50 Auto
4	200803	19.68	536.062	-Z	HIA8147	HB3-50 Auto
5	200803	19.21	416.466	-Z	HIA8155	HB3-50 Auto
6	200803	19.32	520.813	-Z	HIA8156	HB3-50 Auto
7	200703	19.36	504.798	-Z	HIA8094	HB3-50 Auto
8	200703	19.62	402.55	-Z	HIA8131	HB3-50 Auto
9	200703	19.77	565.445	-Z	HIA8232	HB3-50 Auto
10	200703	19.84	530.58	-Z	HIA8233	HB3-50 Auto
11	200703	19.5	665.057	-Z	HIA8234	HB3-50 Auto

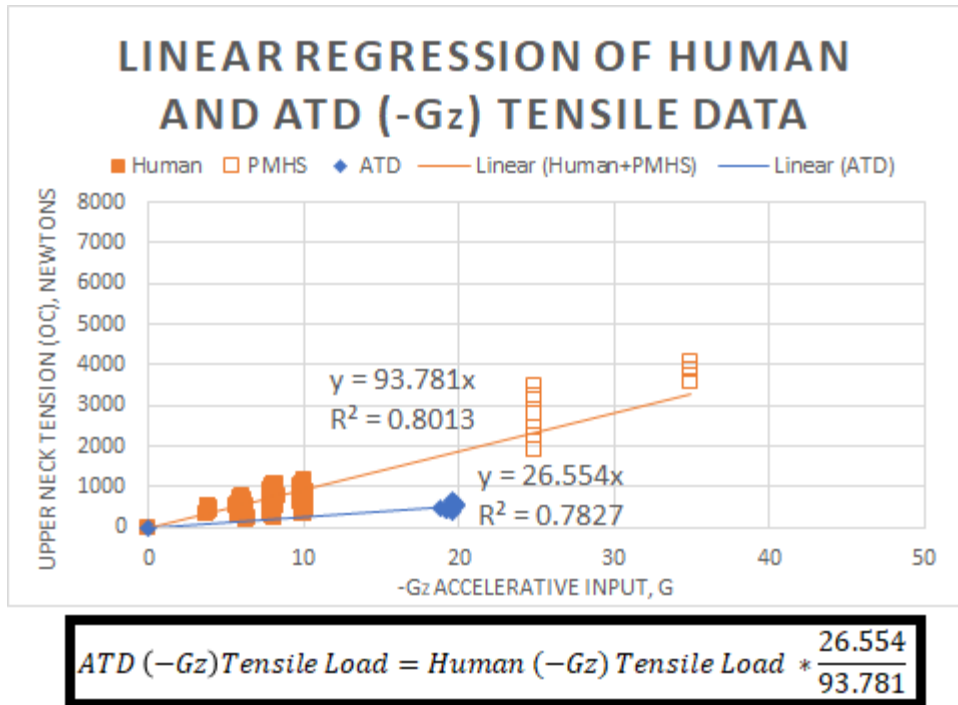


Figure 12. Linear Regression of Human and ATD (-Gz) Tensile Data and (-Gz) Transfer Function

There are a low number of -Gz accelerative ATD test data points available, and they are all from roughly the same accelerative load, but a relationship is still able to be modeled from them. A linear model is successfully fit to the data using a truth point of zero Newtons at zero G accelerative load. A simple linear model of the relationship is supported in this case because the transfer functions created by Zinck (2016) and Satava (2017) were largely linear in nature if the data was from similar subject types as it is in this research (male data points only and with or without a helmet only).

95% Confidence Intervals of Linear Models used in -Gz Transfer Functions

Next, a two-sided 95% confidence interval was calculated for the slope of each linear model to obtain a more and less conservative estimate for the relationship between accelerative level and tensile load. The 95% confidence interval for the slope of the linear model for human -Gz accelerative tests is 93.78 ± 3.623 and the confidence interval for the ATD data is 26.55 ± 2.744 . The most likely estimate linear models, along with their respective 95% confidence interval estimates, are plotted in the figure below.

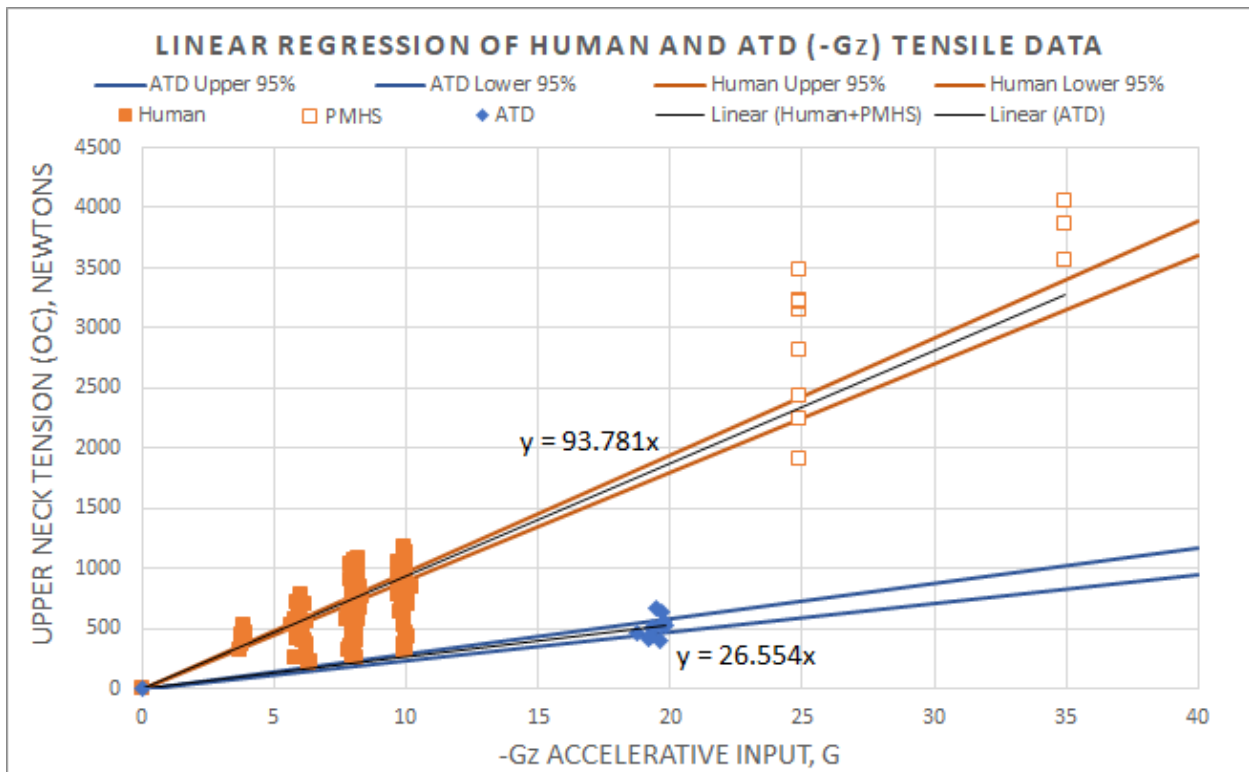


Figure 13. -Gz Linear Regression Models and 95% Confidence Interval Bounds

Using the 95% confidence bounds for each linear model, the largest scale factor would result from using the human upper 95% bound and the ATD lower 95% bound. This scale factor would result in the largest difference in response between human and ATD tensile neck loads

in -Gz accelerative tests. Converting between data types with such a transfer function would constitute a conservative approach to converting tensile neck loads from ATDs. The transfer function using this scale factor is shown in the figure below.

$$ATD (-Gz) Tensile Load = Human (-Gz) Tensile Load * 0.2444$$

Figure 14. -Gz Transfer Function Based on Most Conservative Linear Models

Conversely, the smallest scale factor results from using the lower human 95% bound and the upper ATD 95% bound. This scale factor assumes a smaller difference between human and ATD neck loads in -Gz accelerative tests. Using this scale factor as the transfer function would constitute a less conservative approach to converting tensile neck loads from ATDs. The transfer function using this scale factor is shown in the figure below.

$$ATD (-Gz) Tensile Load = Human (-Gz) Tensile Load * 0.3250$$

Figure 15. -Gz Transfer Function Based on Least Conservative Linear Models

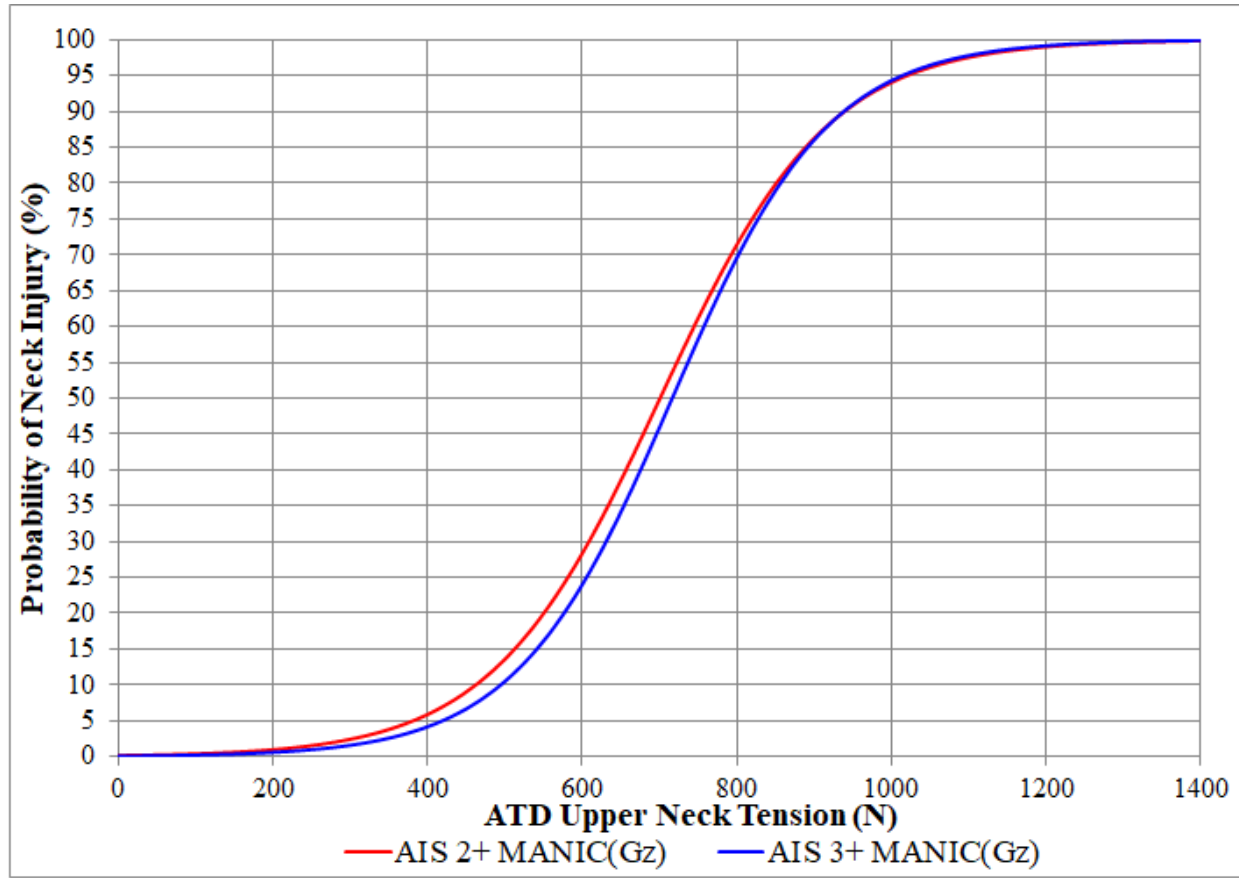
The difference between human and ATD tensile neck loads during -Gz accelerative tests is significant to the application of a tensile neck load criteria to ejection level testing. If an ATD used in an ejection test recorded a peak tensile neck load of 1000 Newtons, it would pass according to the currently accepted value of 1313 Newtons for 5th percentile value for probability of injury. However, using the most and least conservative estimates for the -Gz transfer function, the equivalent tensile neck load experienced by a human would be between 3077-4092 Newtons which would fail the human-based tensile neck injury criteria.

Equivalent ATD Tensile Neck Load Values

The live human, PMHS, and ATD data points introduced above were then converted to equivalent ATD tensile loads using the scale factor method of applying the transfer function specific to their accelerative direction/axis. Appendix B contains the computer code that was used to scale the tensile loads.

Hybrid III 50th Automotive Manikin ATD AIS 2+ and 3+ Risk Curves

The converted tensile neck load data points and their associated injury status were analyzed by survival analysis with an assumed logistic distribution. The computer code used to perform the analysis is shown in Appendix B. The AIS 2+ risk curve is plotted in the figure below and shows a 5th percentile value of 380.9 Newtons (95% CI 268.30 N, 493.6 N). The AIS 3+ risk curve is plotted in the figure below and shows a 5th percentile value of 418.8 N (95% CI 297.4 N, 540.3 N).



$$P(AIS \geq 2) = \frac{1}{1 + \exp\left(\frac{700.6 - \text{Tensile Load}}{108.6}\right)}$$

$$P(AIS \geq 3) = \frac{1}{1 + \exp\left(\frac{716.4 - \text{Tensile Load}}{101.0}\right)}$$

Figure 16. ATD-based Risk Curve Probability of Abbreviated Injury Scale (AIS) 2+ and 3+ after Use of -Gz Tensile Neck Load Transfer Function

Exclusion of PMHS Data from (-Gx) Accelerative Studies

As a note for any future research, the exclusion of the PMHS data points from the -Gx accelerative study currently prevents the creation of an AIS 2+ risk curve as the only AIS 2 data point is from the Cheng (1981) study. The removal of these data points changes the risk curve a

small amount at the 5th percentile and a much larger amount at the 50th percentile. The 5th percentile value is 413.0 Newtons (95% CI 294.9 N, 531.1 N), and the risk curve is plotted in the figure below. The plot has the same x-axis bounds for comparability to the previous risk curve plot.

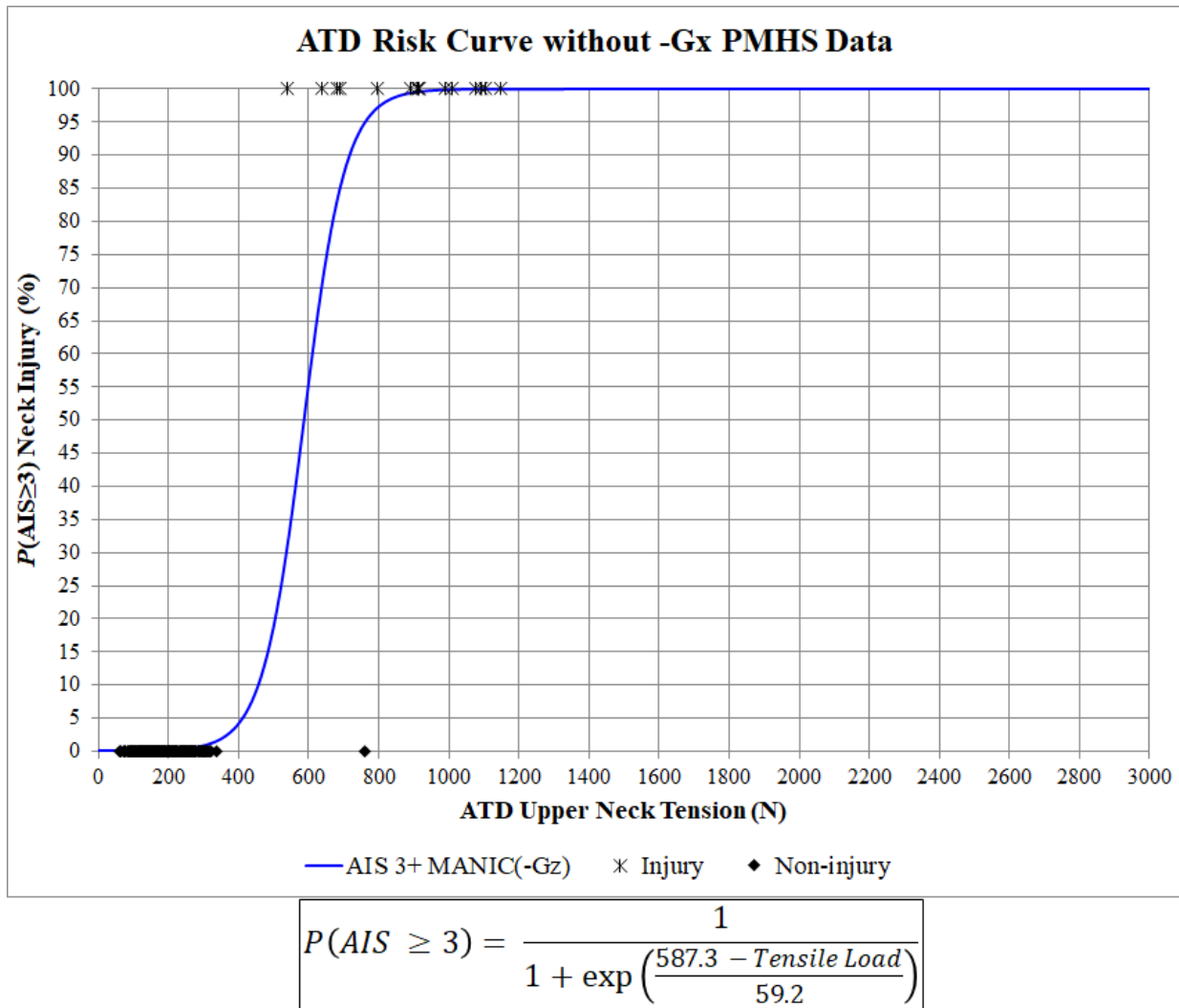


Figure 17. Excluding -Gx PMHS Accelerative Study Data ATD-based Risk Curve Probability of Abbreviated Injury Scale (AIS) 3+ after Use of -Gz Transfer Function

AIS 2+ MANIC(-Gz) Risk Curves Using Transfer Function 95% Confidence Bounds

The most and least conservative scale factors were also used to convert the data types, according to their respective axes, and survival analysis was performed for each scenario. The following figure shows the respective values for the 5th percentile probability of AIS 3+ injury. The more and less conservative estimates differ by approximately 10% from the most likely estimate.

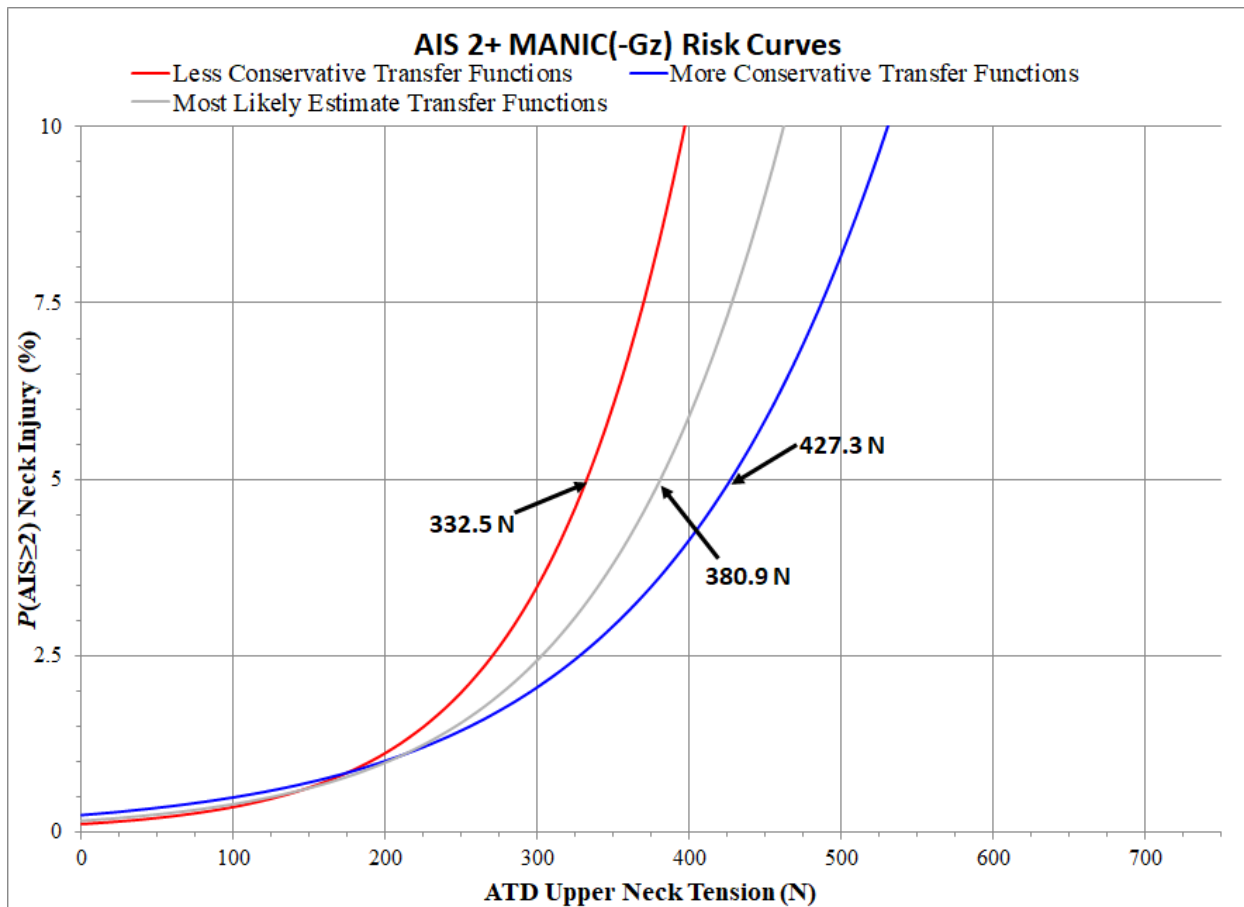


Figure 18. 5% Probability of AIS 2+ Injury After Converting Data Using Most Likely Value and 95% Confidence Interval Bounds for the Transfer Functions

The following table shows the tensile neck load corresponding to the 5% probability of injury for each of the three risk curves. The 95% confidence interval bounds are included as well. Using the least conservative transfer functions and taking the upper 95% CI of the 5th percentile value results in a 559.5 N tensile neck load associated with a 5% probability of AIS 3+ injury. Using the most conservative transfer functions and taking the lower 95% CI of the 5th percentile value results in a 237.3 N tensile neck load associated with a 5% probability of AIS 3+ injury.

Table 11. Most Likely and 95% CI Values of Tensile Neck Load Values Corresponding to the Presented Transfer Functions and the 5% Probability of AIS 2+ Injury

AIS 2+ ATD Risk Curves	Tensile Neck Load Corresponding to 5th Percentile Value, Newtons		
	Lower 95% CI Bound	Most Likely Value	Upper 95% CI Bound
Risk Curve from Using Least Conservative Transfer Functions	295.0	427.3	559.5
Risk Curve from Using Most Likely Transfer Functions	268.3	380.9	493.6
Risk Curve from Using Most Conservative Transfer Functions	237.3	332.5	427.7

AIS 3+ MANIC(-Gz) Risk Curves Using Transfer Function 95% Confidence Bounds

The most and least conservative scale factors were also used to convert the data types, according to their respective axes, and survival analysis was performed for each scenario. The following figure shows the respective values for the 5th percentile probability of AIS 3+ injury. The more and less conservative estimates differ by approximately 10% from the most likely estimate.

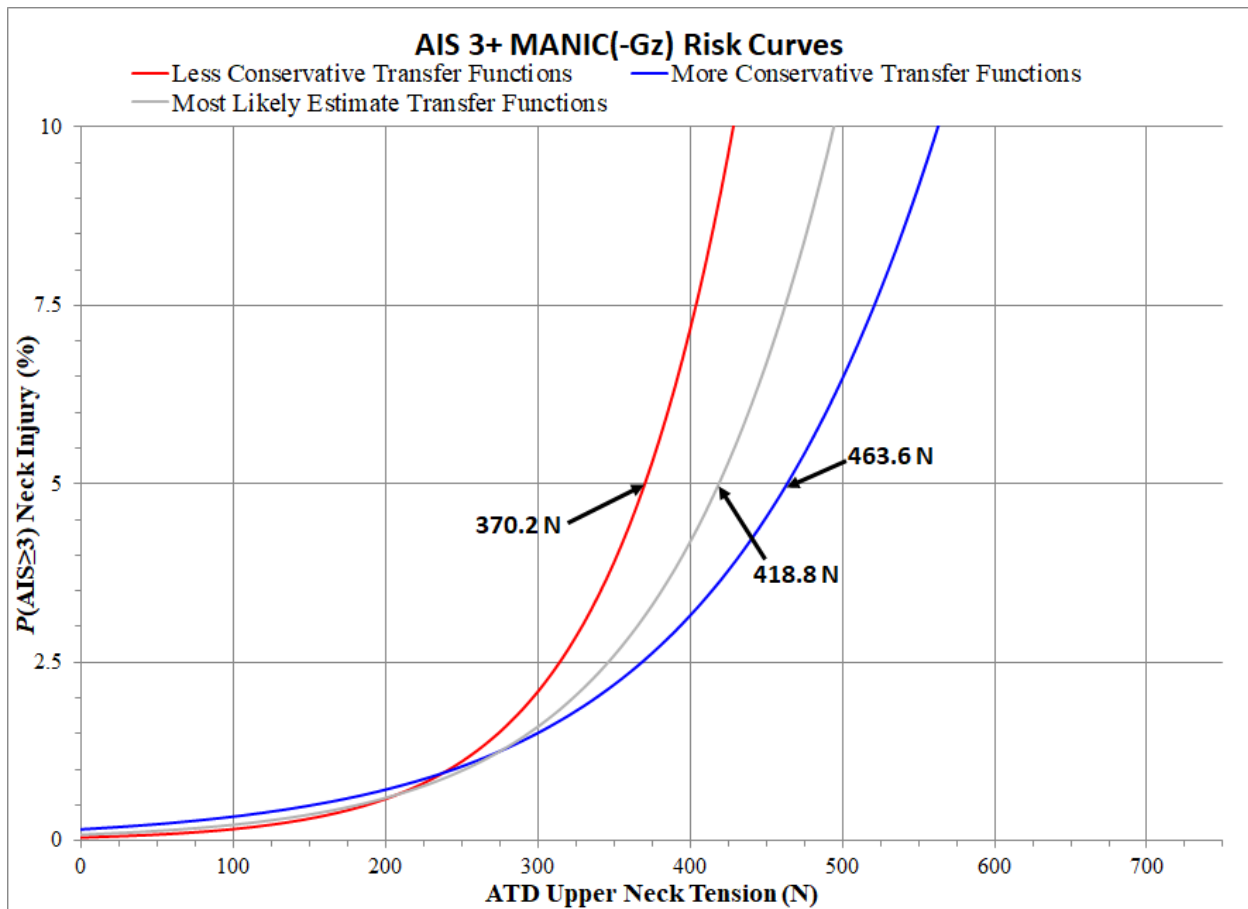


Figure 19. 5% Probability of AIS 3+ Injury After Converting Data Using Most Likely Value and 95% Confidence Interval Bounds for the Transfer Functions

The following table shows the tensile neck load corresponding to the 5% probability of injury for each of the three risk curves. The 95% confidence interval bounds are included as well. Using the least conservative transfer functions and taking the upper 95% CI of the 5th percentile value results in a 559.5 N tensile neck load associated with a 5% probability of AIS 3+ injury. Using the most conservative transfer functions and taking the lower 95% CI of the 5th percentile value results in a 237.3 N tensile neck load associated with a 5% probability of AIS 3+ injury.

Table 12. Most Likely and 95% CI Values of Tensile Neck Load Values Corresponding to the Presented Transfer Functions and the 5% Probability of AIS 3+ Injury

AIS 3+ ATD Risk Curves	Tensile Neck Load Corresponding to 5th Percentile Value, Newtons		
	Lower 95% CI Bound	Most Likely Value	Upper 95% CI Bound
Risk Curve from Using Least Conservative Transfer Functions	323.7	463.6	603.5
Risk Curve from Using Most Likely Transfer Functions	297.4	418.8	540.3
Risk Curve from Using Most Conservative Transfer Functions	265.5	370.2	475.0

V. Conclusions and Recommendations

Research Purpose and Goals

The United States Air Force pilots are equipped with heavy HMDs that increase performance but also increase risk of injury during ejection. To maintain an acceptable level of probability of injury during ejection, qualification ejection level testing must be accomplished with each new HMD and ejection seat. All ejection level testing is conducted with ATDs. However, the neck injury criteria were developed through the combination of human and PMHS data from accelerative tests. Additionally, the biofidelic differences between ATDs and humans have raised concerns that the results from ATD testing are inaccurate and are either constraining the design space for HMDs or are putting the pilots at unacceptable levels of risk of injury. The goal of this research was to develop a transfer function based on human and ATD tensile neck load response due to -Gz accelerative inputs and then create an equivalent AIS 3+ risk curve using converted human/PMHS tensile neck loads and their associated injury status.

Investigative Questions Answered

What is the difference in tensile neck load response between human/PMHS and ATDs over the operational range of accelerative input?

The available data from both -Gz and -Gx accelerative studies show that ATD tensile neck load response is lower than a human or PMHS in an equivalent test. The most likely estimate for the linear model of the data showed that for every 1 G of Z-axis acceleration, humans would experience 93.781 Newtons and ATDs would only experience 26.554 Newtons. Additionally, the data shows that human/PMHS tensile neck loads have an increasing variance as accelerative loads increase and ATD tensile neck loads exhibit nearly constant variance across

the range of accelerative input. One explanation may be the wide range of anthropometric parameters of the human/PMHS data as compared to the identical body types of the ATDs used throughout the tests. However, of the anthropometric parameters and reported in BIODYN, none were found to explain the non-constant variance. As opposed to Satava's (2017) research, the data in this study was not able to be separated into male/female and helmet/no-helmet groupings as all the data was male/male-ATD and not helmeted. The human factor that could explain the non-constant variance could be something much more complicated such as each individual's neck strength or their reaction time.

Are human and ATD neck load responses significantly different and does the difference justify the need for a transfer function?

The difference in linear models indicates that the mechanics of human and ATD necks operate significantly differently during -Gz accelerative input. The data indicates that when ATDs are used in ejection testing, their tensile neck load response will be significantly lower than what a human would experience and the ATD data should not be used directly. The MANIC(-Gz) neck injury criteria is based on the 5th percentile value from a human-data based risk curve (as shown in Chapter 4); a value of 1367.6 Newtons. However, the linear models indicate that an ATD that reports a tensile neck load of 1367.6 Newtons would be reporting a value corresponding to a much higher probability of AIS 3+ injury for a human in the same ejection event. The tensile neck load data collected from ATDs in accelerative and ejection tests should not be used to calculate a probability of injury for a human without first being converted with a transfer function.

What is an appropriate transfer function for making human-based -Gz risk curves, developed by Parr (2014), and associated neck injury criterion more appropriate for ejection system testing with ATDs?

A transfer function that proportionally scales values between the linear models should be used by multiplying (or dividing, as appropriate) the proportion of linear model coefficients by the tensile load of one data type to convert to an equivalent value for the other data type. A scale factor method (through multiplication/division) converts the tensile neck loads proportionally between the different linear models for each data type. Additionally, any tensile load can be converted between data types as a scale factor transfer method does not require an associated accelerative level. This is because both relationships are linear models with a (0,0) intercept and thus are at a constant proportional difference across all accelerative levels. The most likely value for the transfer function is shown in the figure below.

$$ATD (-Gz)Tensile Load = Human (-Gz)Tensile Load * 0.2831$$

Figure 20. Most Likely Value for the Tensile Neck Load Transfer Function for -Gz Accelerative Input

The 95% confidence interval on the slope of the linear models used to create the -Gz transfer function provide more and less conservative bounds for the scale factor. The -Gz transfer functions using each of those scale factors are shown below.

$$ATD (-Gz)Tensile Load = Human (-Gz)Tensile Load * 0.3250$$

Figure 21. More Conservative Value for the Tensile Neck Load Transfer Function for -Gz Accelerative Input

$$ATD (-GZ)Tensile Load = Human (-GZ) Tensile Load *0.2444$$

Figure 22. Less Conservative Value for the Tensile Neck Load Transfer Function for -Gz Accelerative Input

If a transfer function is appropriate, what is the equivalent ATD MANIC (-Gz) risk curve that would provide an equivalent 5th percentile probability of AIS 2+ and 3+ injury for ATD tensile neck loads during ejection tests?

After the conversion of human and PMHS data points to equivalent ATD data points and maintaining their associated injury status, survival analysis was accomplished, and a risk curve was defined. The 5th percentile value on the ATD MANIC(-Gz) risk curve is 380.9 Newtons and the risk curve and its equation are shown in the figure below. This is the most likely value and was shown on the curve in the center of Figure 17 in Chapter 4.

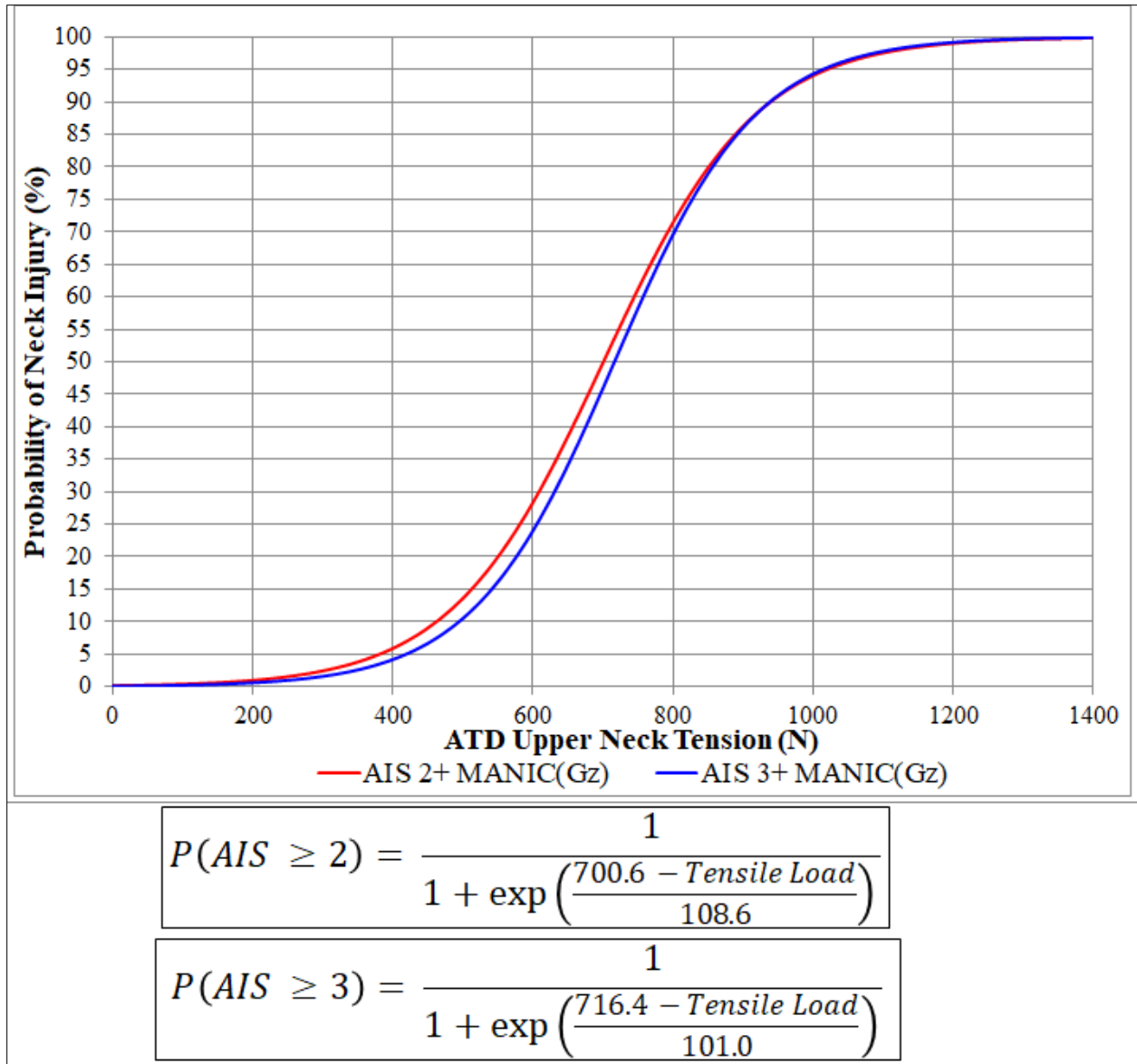


Figure 23. ATD-based Risk Curve Probability of Abbreviated Injury Scale (AIS) 3+ after Use of Most Likely Value of Transfer Functions

The most likely values are recommended to be used. However, subject matter experts should decide between the values shown in Table 11 because the highest and lowest tensile neck loads in an ATD associated with a 5% probability of injury range from 237.3-559.5 N. This range is significant and differs significantly from the human-data based limit of 1367.6 N.

Recommendations for Future Work

Additional -Gz accelerative tests should be accomplished for live humans, PMHS, and ATDS. The live human testing be accomplished with the current operational ejection seats and HMDs. The PMHS testing should be accomplished as accelerative sled tests with an associated accelerative level between 10-25 Gs to fill in that gap of data that would further the accuracy of the estimate of probability of injury. Information theory supports testing at the accelerative level where PMHS would be at 50% probability injury at the chosen AIS injury level. Based on this research, that range would be somewhere within the 19-28 G range. Testing at the 50% probability level has the highest likelihood of providing the most information according to the binary entropy function. The ATD testing should be accomplished with current operation ejection seats and HMDs to improve the relevance of the data; additionally, the tests should be at a range of accelerative levels such as 5, 10, 15, 20, 25, and 35 Gs to verify the models shown in this research.

Once additional -Gz accelerative testing is completed, future research can focus on determining other explanatory factors in Z-axis accelerative tests such as the effect of pilot weight, helmet weight, and gender on the relationship between accelerative load and tensile neck load. The potential differences in each group's relationship between -Gz accelerative load and tensile neck load would refine the transfer function's accuracy.

Additional follow on research should focus on the use of a newly built ejection seat for vertical accelerative testing with ATDs, humans, and PMHS. The seat can change seat angles and configurations which are important parts of the data that needs to be collected. PMHS neck

load data from these accelerative tests can be used to improve the MANIC Z-axis component. Currently, the Z-axis component of the MANIC only considers tensile neck load (Parr, 2014). +Gz largely correlates with compressive neck load and can be accounted for in a new MANIC(Gz) once this data is collected.

**Appendix A: Live Human Data from -Gz Accelerative Studies Used in
Creating -Gz Transfer Function**

Study Number	Peak Accelerative Load, G	Tension, N	Censor	AIS 3+ Injury	
1	198504	3.78	375.5488	R-censored	No
2	198504	3.75	324.446	R-censored	No
3	198504	3.93	454.6817	R-censored	No
4	198504	3.85	516.2146	R-censored	No
5	198504	3.83	428.2745	R-censored	No
6	198504	3.82	449.2605	R-censored	No
7	198504	3.92	462.8287	R-censored	No
8	198504	3.87	437.6172	R-censored	No
9	198504	3.87	525.7767	R-censored	No
10	198504	3.91	452.1475	R-censored	No
11	198504	3.85	450.8057	R-censored	No
12	198504	5.68	528.6153	R-censored	No
13	198504	6.21	700.2934	R-censored	No
14	198504	5.95	662.52	R-censored	No
15	198504	6.01	779.9055	R-censored	No
16	198504	6.26	291.116	R-censored	No
17	198504	6.36	228.6944	R-censored	No
18	198504	6.29	210.8418	R-censored	No
19	198504	5.78	584.3562	R-censored	No
20	198504	5.89	719.8461	R-censored	No
21	198504	3.84	486.6795	R-censored	No
22	198504	6.02	701.5413	R-censored	No
23	198504	6.06	740.1893	R-censored	No
24	198504	6	472.94	R-censored	No
25	198504	5.82	265.1005	R-censored	No
26	198504	5.87	426.8459	R-censored	No
27	198504	5.87	472.1629	R-censored	No
28	198504	5.91	418.9759	R-censored	No
29	198504	6.19	408.1115	R-censored	No
30	198504	6.23	370.3987	R-censored	No
31	198504	8.01	276.0574	R-censored	No
32	198504	8.06	370.7511	R-censored	No
33	198504	8.11	253.5861	R-censored	No
34	198504	8.06	315.4129	R-censored	No
35	198504	8.05	270.2376	R-censored	No
36	198504	7.99	334.6772	R-censored	No
37	198504	8.03	342.2254	R-censored	No
38	198504	8.06	329.2073	R-censored	No
39	198504	7.87	324.0188	R-censored	No
40	198504	8.06	377.1929	R-censored	No

41	198504	7.94	349.3549	R-censored	No
42	198504	8.04	404.2636	R-censored	No
43	198504	7.96	613.9176	R-censored	No
44	198504	7.95	510.5483	R-censored	No
45	198504	7.93	644.714	R-censored	No
46	198504	7.96	595.6574	R-censored	No
47	198504	8.06	487.4809	R-censored	No
48	198504	7.99	486.8145	R-censored	No
49	198504	8.11	537.7957	R-censored	No
50	198504	7.8	573.4658	R-censored	No
51	198504	8.04	479.1539	R-censored	No
52	198504	8.09	513.8463	R-censored	No
53	198504	8.13	851.4126	R-censored	No
54	198504	8.12	756.4948	R-censored	No
55	198504	8.11	707.2204	R-censored	No
56	198504	8.11	667.7781	R-censored	No
57	198504	8.06	970.4112	R-censored	No
58	198504	8.12	887.1132	R-censored	No
59	198504	8.05	858.9784	R-censored	No
60	198504	8.08	884.953	R-censored	No
61	198504	7.96	564.3379	R-censored	No
62	198504	7.87	676.8883	R-censored	No
63	198504	8.02	649.6094	R-censored	No
64	198504	8	720.3526	R-censored	No
65	198504	7.93	1036.605	R-censored	No
66	198504	7.95	888.4869	R-censored	No
67	198504	7.88	908.3542	R-censored	No
68	198504	7.96	836.3686	R-censored	No
69	198504	7.95	865.9638	R-censored	No
70	198504	7.95	941.3491	R-censored	No
71	198504	7.99	920.1343	R-censored	No
72	198504	7.86	622.3169	R-censored	No
73	198504	3.89	508.4998	R-censored	No
74	198504	8.27	670.6405	R-censored	No
75	198504	8.31	774.702	R-censored	No
76	198504	8.12	948.0673	R-censored	No
77	198504	8.23	1091.795	R-censored	No
78	198504	8.18	868.6503	R-censored	No
79	198504	8.24	829.4486	R-censored	No
80	198504	8.26	847.9346	R-censored	No
81	198504	8.11	1068.421	R-censored	No
82	198504	8.1	789.2976	R-censored	No
83	198504	8.14	815.1896	R-censored	No

84	198504	8.2	1006.903	R-censored	No
85	198504	8.19	932.9772	R-censored	No
86	198504	3.85	455.5267	R-censored	No
87	198504	8.11	403.666	R-censored	No
88	198504	8.15	522.2854	R-censored	No
89	198504	8.08	461.6234	R-censored	No
90	198504	8.09	630.0843	R-censored	No
91	198504	8.17	579.5337	R-censored	No
92	198504	8.15	529.1057	R-censored	No
93	198504	8.16	598.3927	R-censored	No
94	198504	8.16	527.5264	R-censored	No
95	198504	8.14	696.3012	R-censored	No
96	198504	8.13	558.4175	R-censored	No
97	198504	8.14	514.3775	R-censored	No
98	198504	6.26	553.5321	R-censored	No
99	198504	8.09	857.485	R-censored	No
100	198504	8.03	1061.885	R-censored	No
101	198504	6.01	580.6086	R-censored	No
102	198504	7.88	640.8333	R-censored	No
103	198504	8.05	550.9252	R-censored	No
104	198504	7.98	443.4082	R-censored	No
105	198504	8.02	457.8095	R-censored	No
106	198504	7.98	504.619	R-censored	No
107	198504	8	763.4131	R-censored	No
108	198504	7.97	650.9905	R-censored	No
109	198504	7.96	884.2233	R-censored	No
110	198504	7.94	660.4634	R-censored	No
111	198504	8.05	584.1209	R-censored	No
112	198504	7.99	729.2076	R-censored	No
113	198504	8.03	682.8872	R-censored	No
114	198504	8.04	614.1494	R-censored	No
115	198504	8	649.8089	R-censored	No
116	198504	9.87	1005.273	R-censored	No
117	198504	9.86	902.5919	R-censored	No
118	198504	10	1074.543	R-censored	No
119	198504	9.98	1133.233	R-censored	No
120	198504	9.76	845.2039	R-censored	No
121	198504	9.74	780.7424	R-censored	No
122	198504	10.03	323.387	R-censored	No
123	198504	9.74	843.2975	R-censored	No
124	198504	9.82	954.943	R-censored	No
125	198504	9.74	970.861	R-censored	No
126	198504	9.87	832.3026	R-censored	No

127	198504	10.03	791.258	R-censored	No
128	198504	10.1	862.3943	R-censored	No
129	198504	9.91	733.7588	R-censored	No
130	198504	9.93	707.9089	R-censored	No
131	198504	9.81	891.3974	R-censored	No
132	198504	10.08	778.0218	R-censored	No
133	198504	9.86	980.5798	R-censored	No
134	198504	9.84	1057.921	R-censored	No
135	198504	10.12	853.223	R-censored	No
136	198504	9.99	1084.37	R-censored	No
137	198504	9.94	558.8906	R-censored	No
138	198504	9.96	336.8296	R-censored	No
139	198504	9.92	321.4348	R-censored	No
140	198504	9.94	940.346	R-censored	No
141	198504	9.93	983.4232	R-censored	No
142	198504	9.82	923.9123	R-censored	No
143	198504	9.98	793.6188	R-censored	No
144	198504	9.91	543.3821	R-censored	No
145	198504	10.01	323.6691	R-censored	No
146	198504	10.04	359.4309	R-censored	No
147	198504	10.1	441.3032	R-censored	No
148	198504	10	434.9748	R-censored	No
149	198504	9.92	362.6392	R-censored	No
150	198504	9.98	324.5611	R-censored	No
151	198504	10.03	470.0001	R-censored	No
152	198504	9.79	855.7388	R-censored	No
153	198504	9.89	855.4141	R-censored	No
154	198504	9.97	1187.822	R-censored	No
155	198504	9.94	908.2897	R-censored	No
156	198504	9.98	1126.198	R-censored	No
157	198504	10.03	1024.705	R-censored	No
158	198504	9.92	637.962	R-censored	No
159	198504	9.92	528.6824	R-censored	No
160	198504	9.92	600.243	R-censored	No
161	198504	9.93	553.7576	R-censored	No
162	198504	9.87	767.7025	R-censored	No
163	198504	9.85	854.2053	R-censored	No
164	198504	10.04	1108.33	R-censored	No
165	198504	10.21	854.3286	R-censored	No
166	198504	9.75	1046.349	R-censored	No
167	198504	9.97	723.2396	R-censored	No
168	198504	10	1013.637	R-censored	No
169	198504	9.76	641.067	R-censored	No

170	198504	9.85	759.0325	R-censored	No
171	198504	9.83	944.6569	R-censored	No
172	198504	9.87	834.6203	R-censored	No
173	198504	9.91	625.1775	R-censored	No
174	198504	9.95	957.1989	R-censored	No
175	198504	6.13	485.3072	R-censored	No
176	198504	5.88	478.6438	R-censored	No
177	198504	6.07	541.7571	R-censored	No
178	198504	5.94	462.6592	R-censored	No
179	198504	5.94	606.9615	R-censored	No
180	198504	5.95	612.4381	R-censored	No
181	198504	6.13	394.4204	R-censored	No
182	198504	6	545.8746	R-censored	No
183	198504	7.99	668.979	R-censored	No
184	198504	8.06	594.106	R-censored	No
185	198504	7.98	769.3864	R-censored	No
186	198504	8	850.5976	R-censored	No
187	198504	7.98	656.0195	R-censored	No
188	198504	5.95	505.6476	R-censored	No
189	198504	8.06	709.2739	R-censored	No
190	198504	7.98	881.6702	R-censored	No
191	198504	8.06	545.8717	R-censored	No
192	198504	10.03	927.8926	R-censored	No
193	198504	10.03	840.62	R-censored	No
194	198504	9.89	759.7561	R-censored	No
195	198504	9.91	895.4392	R-censored	No
196	198504	8.06	560.2859	R-censored	No
197	198504	10.03	734.1136	R-censored	No
198	198504	9.93	786.6002	R-censored	No
199	198504	10.09	696.1949	R-censored	No
200	198504	10.03	749.241	R-censored	No

Appendix B: Computer Code to Convert Human/PMHS (-Gz) and (-Gx) Data to Equivalent ATD Data and Perform Survival Analysis

```
library(SMRD)
options("digits" = 15)
```

```
#MANIC(-Gz) transfer function from Human to ATD is
#Human Tension Value * (26.554/93.781) = ATD Tension Value, along w/ assoc. injury status
```

```
#First convert live human tension values, Newtons
```

```
Human <- c(210.841756939273, 228.694389845978, 253.586080941635, 265.100544457864,
270.237641074249, 276.057436129785, 291.115999300476, 315.412889402234,
321.434780707373, 323.387020297369, 323.669140553113, 324.018795911578,
324.445997857843, 324.561112967609, 329.207256536993, 334.677192610638,
336.829594027698, 342.225377237299, 349.354946038794, 359.430911867041,
362.639236493195, 370.398748298071, 370.751118635541, 375.548825907819,
377.192915380872, 394.420441340546, 403.666030840448, 404.263631656445,
408.111469586969, 418.975899255188, 426.845910705524, 428.274498720142,
434.974761466644, 437.617216593909, 441.303207838562, 443.408164997528,
449.260505863873, 450.805702226709, 452.147512724915, 454.681674127161,
455.526745279364, 457.809499625849, 461.623434256061, 462.659198746051,
462.82868131037, 470.000060788525, 472.162948811987, 472.94004367738,
478.643841254974, 479.153917935333, 485.307180287024, 486.679534299023,
486.814536629993, 487.480860352027, 504.618961690759, 505.647633298102,
508.499786616181, 510.54834008634, 513.846326894098, 514.377512536212,
516.214603079205, 522.285397943652, 525.776691256488, 527.526393412793,
528.615337554022, 528.682363598181, 529.105730636603, 537.795665746118,
541.757091610718, 543.382142293506, 545.87174410285, 545.874594830804,
550.925168460059, 553.532057362372, 553.757638180359, 558.417526330951,
558.890577485144, 560.285907006964, 564.337877421344, 573.465806518665,
579.53371671792, 580.608644780042, 584.120877368445, 584.356198173609,
594.105959274536, 595.657434026319, 598.392707498279, 600.243033563916,
606.961452732507, 612.438108379187, 613.917636187366, 614.149427519824,
622.316898857275, 625.177468610266, 630.084318038501, 637.961965367285,
640.833327161816, 641.066951105102, 644.71398240105, 649.609428917468,
649.80891199978, 650.99047086228, 656.019494345691, 660.463439853759,
662.519968574744, 667.778068411609, 668.978971499512, 670.640470775427,
676.888316208167, 682.887198066247, 696.194939151794, 696.301162705322,
700.293403581616, 701.541343680762, 707.220401012183, 707.908919687573,
709.273943256262, 719.846071497473, 720.352550830652, 723.239591628931,
729.207590600842, 733.75884565404, 734.113557660901, 740.189341299267,
749.241013423816, 756.494758577503, 759.032517326929, 759.75605923147,
763.413068075257, 767.702531278003, 769.386429130701, 774.701950773499,
778.021759225, 779.905479532385, 780.742439684814, 786.600210509167,
```

```
789.297610024023, 791.258028488269, 793.618838481116, 815.189550290576,
829.448552144617, 832.302605947998, 834.620315649158, 836.368626378723,
840.62001200094, 843.297524294592, 845.20391467666, 847.934640558789,
850.597559840296, 851.412596537268, 853.223012411548, 854.205291815161,
854.328619736414, 855.414068342175, 855.738847705517, 857.48498645188,
858.978428527454, 862.394347235694, 865.963798006604, 868.650269730969,
881.670155167627, 884.223253548425, 884.953039904675, 887.113212949133,
888.486924450635, 891.397381942822, 895.439171185938, 902.591919120679,
908.289709807227, 908.354190558569, 920.134348707569, 923.912309865979,
927.892604834656, 932.977217513171, 940.346009902148, 941.349058895142,
944.656921439026, 948.067274440308, 954.9429587677, 957.198902696521,
970.411212270081, 970.861016416553, 980.579826756836, 983.423156393152,
1005.27330741659, 1006.90290568921, 1013.63680023812, 1024.70529451572,
1036.60504748984, 1046.34910713486, 1057.92143364111, 1061.88503148892,
1068.4214113153, 1074.54294234988, 1084.37001247794, 1091.79480130887,
1108.32997368532, 1126.19847225057, 1133.23264347732, 1187.82245481096)
```

```
ATD.human <- Human * (26.554/93.781)
```

```
#All of the live human tests resulted in no injuries
```

```
ATD.human.cens <- rep('R-censored',length(ATD.human))
```

```
#Next convert PMHS -Gz test tension values, Newtons
```

```
PMHS.z <- c(3560, 4060, 3860, 2250, 1910, 2810, 3150, 3230, 3220, 2440,
           3230, 3490, 2400, 3900, 3800, 2688)
```

```
ATD.PMHS.z <- PMHS.z * (26.554/93.781)
```

```
#MANIC(-Gx) transfer function from Human to ATD is
```

```
#Human Tension Value * (28.966/80.289) = ATD Tension Value, along w/ assoc. inj status
```

```
#Next convert PMHS -Gx test tension values, Newtons
```

```
PMHS.x <- c(3490, 7200, 850, 2420, 6520, 3210)
```

```
ATD.PMHS.x <- PMHS.x * (28.966/80.289)
```

```
#Combine converted PMHS data points
```

```
ATD.PMHS <- c(ATD.PMHS.z, ATD.PMHS.x)
```

```
ATD.PMHS.cens <- c(rep("L-censored", 12), rep("L-censored", 3), "R-censored",
                 rep("L-censored", 3), "R-censored", "L-censored", "R-censored")
```

```
ATD.loads <- c(ATD.human,ATD.PMHS)
```

```
ATD.cens <- c(ATD.human.cens,ATD.PMHS.cens)
```

```
ATD.data <- data.frame(ATD.loads,ATD.cens)
```



```
ATD.data.ld <- frame.to.ld(ATD.data,response.column = 1, censor.column = 2)
ATD.params <- print(mlest(data.ld = ATD.data.ld, distribution = 'logistic'))$mle.table
```

```
#5th percentile value of tension for the ATD risk curve, Newtons
qlogis(0.05, location = ATD.params[1, 1], scale = ATD.params[2, 1])
```

```
#95% CI on 5th quantile is found by running this line of code
print(mlest(data.ld = ATD.data.ld, distribution = 'logistic'))$quantiles[4, c(4, 5)]
```

```
#In the logistic distribution equation, mu is found by running this line of code
ATD.params[1, 1]
#and sigma is found by running this line of code
ATD.params[2, 1]
```

Bibliography

APP Business Plan for FY15-24 (8 Feb 2017) Final_CEP_CWP_JB.

Association for the Advancement of Automotive Medicine (AAM). (2017) *Abbreviated Injury Scale Overview*. Retrieved from <https://www.aaam.org/abbreviated-injury-scale-ais/>

Bass, C., Donnellan, L., Salzar, R., Lucas, S., Folk, B., Davis, M., Rafaels, K., Planchak, C., Meyerhoff, K., Ziemba, A., Alem, N. (2006). "A New Neck Injury Criterion in Combined Vertical/Frontal Crashes with Head Supported Mass." 2006 International IRCOBI Conference on the Biomechanics of Impact. Madrid, Spain.

Bennett, Michael. Project Get Out and Walk. 1980 – 2009. <http://www.ejection-history.org.uk/>

Bredbenner, T. L., Eliason, T. D., Francis, W. L., McFarland, J. M., Merkle, A. C., Nicolella, D.P. (2013). "Development and Validation of a Statistical Shape Modeling-Based Finite Element Model of the Cervical Spine Under Low-Level Multiple Direction Loading Conditions". *Frontiers in Bioengineering and Biotechnology*: doi: 10.3389/fbioe.2014.00058.

Buhrman, J.R. and Perry, C.E. (1994). "Human and Manikin Head/Neck Response to +Gz Acceleration When Encumbered by Helmets of Various Weights." *Aviation, Space, and Environmental Medicine*: 1086-1090.

Cheng, R., Yang, K.H., Levine, R.S., King, A.I., & Morgan, R. (1982). "Injuries to the Cervical Spine Caused by a Distributed Frontal Load to the Chest." SAE International: Warrendale, PA: SAE Paper No. 821155.

Chancey, C.V., Ottaviano, D., Myers, B.S., & Nightingale, R.W. (2007). "A Kinematic and Anthropometric Study of the Upper Cervical Spine and the Occipital Condyles." *Journal of Biomechanics*: 40: 1953-1959.

Doczy, E., Mosher, S., & Buhrman, J. (2004). "The Effects of Variable Helmet Weight and Subject Bracing on Neck Loading During Frontal -Gx Impact." *Proceedings of the 42nd Annual SAFE Symposium*. Salt Lake City.

EZFC-CSB-16-001, USAF Revision of MIL-HDBK-516C Section 9.1.1 Escape System Safety Compatibility Criteria Standard; Supporting Data And Legacy Criteria. 16 Nov 2016. AFLCMC/EZFC

Federal Aviation Administration (FAA). (2011). Neck injury criteria for side-facing aircraft seats. Washington, DC: Federal Aviation Administration.

- Gallagher, H. Buhman, J. Perry, C. (2007). An Analysis of Vertebral Stress and BMD During +Gz Impact Accelerations. Wright-Patterson AFB, OH: Air Force Research Laboratory. Report No. AFRL-HE-WP-TR-2007-0085.
- Herbst, B., Forrest, S., Chng, D., & Sances, A. (1998). Fidelity of Anthropometric Test Dummy Necks in Rollover Accidents. National Highway Traffic Safety Administration. Paper No. 98-S9-W-20. Retrieved from <https://www-nrd.nhtsa.dot.gov/pdf/Esv/esv16/98S9W20.PDF>
- Meeker, William Q., Luis A. Escobar, and Jason K. Freels (2015). SMRD: Statistical Methods for Reliability Data. R package version 0.9.1.
- Montgomery, D, Peck, E., & Vining, G. (2006). Introduction to Linear Regression Analysis. Hoboken, NJ: John Wiley & Sons, Inc.
- Nichols, J. (2006). "Overview of Ejection Neck Injury Criteria." Proceedings of the 44th Annual SAFE Symposium, 159-171.
- Parr, J. (2014). "A Method To Develop Neck Injury Criteria To Aid Design And Test Of Escape Systems Incorporating Helmet Mounted Displays." Doctoral Dissertation, Air Force Institute of Technology. Dayton, OH
- Parr, J. C., Miller, M. E., Pellettiere, J. A., & Erich, R. A. (2013). Neck injury criteria formulation and injury risk curves for the ejection environment: A pilot study. *Aviation, Space, and Environmental Medicine*, 84(12), 1240–1248.
- Parr, J. C., Miller, M. E., Schubert Kabban, C. M., Pellettiere, J. A., & Perry, C. E. (2014). Development of an updated tensile neck injury criterion. *Aviation, Space, and Environmental Medicine*, 85(10), 1026–1032.
- Parr, J., Miller, M., Colombi, J., Shubert Kabban, C., & Pellettiere, J. (2015). "Development of a Side-Impact (Gy) Neck Injury Criterion for Use in Aircraft and Vehicle Safety Evaluation." *IIE Transactions on Occupational Ergonomics and Human Factors*: 3 (4), 151–164.
- Perry, C. (1998). "The Effect of Helmet Inertial Properties on Male and Female Head Response During +Gz Impact Accelerations." *SAFE Journal*: 28(1): 32-38.
- RStudio Team (2015). RStudio: Integrated Development for R. RStudio, Inc., Boston, MA. <http://www.rstudio.com/>.
- Satava, S. (2017). "Neck Injury Criteria Development for Use in System Level Ejection Testing; Characterization of ATD to Human Response Correlation Under Gy Accelerative Input." Master's Thesis, Air Force Institute of Technology. Dayton, OH.

- Seemann, M., Muzzy, W., & Lustick, L. (1986). Comparison of Human and Hybrid III Head and Neck Dynamic Response. SAE Technical Paper No. 861892, 1986. doi: 10.4271/861892
- Seligman, L. (2015, October 14). *USAF Acknowledges Expanded Risk of Neck Damage to F-35 Pilots*. Retrieved from: <http://www.defensenews.com/story/breaking-news/2015/10/14/f-35s-heavier-helmet-complicates-ejection-risks/73922710/>.
- Specker, L. J., and Plaga, J. A., 1996, "The K-36D Ejection Seat Foreign Comparative Testing (FCT) Program". Armstrong Lab Wright-Patterson AFB, Report No. AL/CF-TR-1996-0099.
- Spittle, E., Shipley, B., & Kaleps, I. (1992). Hybrid II and Hybrid III Dummy Neck Properties for Computer Modeling. Wright-Patterson AFB, OH: Armstrong Laboratory. Report No. AL-TR-1992-0049.
- Yliniemi EM, Pelletiere J, Doczy E, Nuckley D, Perry C, Ching R. "Dynamic tensile failure mechanics of the musculoskeletal neck using a cadaver model". J Biomech Eng 2009; 131:051001.19.
- Yoganandan, N., Pintar, F., Maiman, D., Cusick, J., Sances, A., Walsh, P. (1996). "Human Head-Neck Biomechanics Under Axial Tension." Medical Engineering and Physics: 18: 289-294.
- Zinck, C. (2016). "Neck injury criteria development for use in system level ejection testing; Characterization of ATD to Human response correlation under -Gx accelerative input." Master's Thesis, Air Force Institute of Technology. Dayton, OH.

REPORT DOCUMENTATION PAGE			Form Approved OMB No. 0704-0188		
The public reporting burden for this collection of information is estimated to average 1 hour per response, including the time for reviewing instructions, searching existing data sources, gathering and maintaining the data needed, and completing and reviewing the collection of information. Send comments regarding this burden estimate or any other aspect of this collection of information, including suggestions for reducing this burden to Department of Defense, Washington Headquarters Services, Directorate for Information Operations and Reports (0704-0188), 1215 Jefferson Davis Highway, Suite 1204, Arlington, VA 22202-4302. Respondents should be aware that notwithstanding any other provision of law, no person shall be subject to any penalty for failing to comply with a collection of information if it does not display a currently valid OMB control number. PLEASE DO NOT RETURN YOUR FORM TO THE ABOVE ADDRESS.					
1. REPORT DATE (DD-MM-YYYY) 23-03-2018		2. REPORT TYPE Master's Thesis		3. DATES COVERED (From — To) Aug 2016 – March 2018	
4. TITLE AND SUBTITLE Characterization of ATD and Human Responses Under -Gz Accelerative Input			5a. CONTRACT NUMBER		
			5b. GRANT NUMBER		
			5c. PROGRAM ELEMENT NUMBER		
6. AUTHOR(S) Berry, Joe, R. Captain, USAF			5d. PROJECT NUMBER		
			5e. TASK NUMBER		
			5f. WORK UNIT NUMBER		
7. PERFORMING ORGANIZATION NAME(S) AND ADDRESS(ES) Air Force Institute of Technology Graduate School of Engineering and Management (AFIT/EN) 2950 Hobson Way WPAFB OH 45433-7765			8. PERFORMING ORGANIZATION REPORT NUMBER AFIT-ENV-MS-18-M-178		
			9. SPONSORING / MONITORING AGENCY NAME(S) AND ADDRESS(ES) Dr. Casey Pirstill and Mr. John Buhrman 2800 Q Street, Bldg. 824, Rm 142 Wright-Patterson AFB OH 45433-7947		
			11. SPONSOR/MONITOR'S REPORT NUMBER(S)		
12. DISTRIBUTION / AVAILABILITY STATEMENT DISTRIBUTION STATEMENT A. APPROVED FOR PUBLIC RELEASE; DISTRIBUTION UNLIMITED					
13. SUPPLEMENTARY NOTES This material is declared a work of the U.S. Government and is not subject to copyright protection in the United States.					
14. ABSTRACT Modern Helmet Mounted Displays (HMD) provide pilots with increased operational capabilities that are essential. Increasing HMD mass in addition to the Air Force's (AF) expanded range of accepted pilot size increases the risk for neck injuries during ejection. This increase drove Parr et al. (2014) to develop improved neck injury criteria, the MANIC, that increases objective interpretation of ejection system qualification testing results and provides early input to HMD and escape system design. The criteria's defined human risk curves provide clear implementation guidance for the MANIC with the Air Force Life Cycle Management Center's (AFLCMC) requirement for ejection systems to maintain risk of AIS 2+ injury below 5%. All AF ejection systems use Anthropometric Test Devices (ATD) for proof of concept and full system developmental testing. Kinematic differences between human and ATD MANIC responses to accelerative input necessitate a transfer function for ATD data before utilizing the MANIC. This study generates a human to ATD transfer function for the MANIC Gz using linear regression and statistical analysis. The development of a transfer function makes human-centric neck injury criterion directly applicable to dynamic testing with ATDs as part of the developmental and operational testing of escape systems and HMDs.					
15. SUBJECT TERMS Helmet Mounted Display, Neck Injury, Ejection, Testing, MANIC, Tension, Tensile					
16. SECURITY CLASSIFICATION OF:			17. LIMITATION OF ABSTRACT UU	18. NUMBER OF PAGES 71	19a. NAME OF RESPONSIBLE PERSON Lt Col Jeffrey C. Parr, PhD, AFIT/ENV
a. REPORT U	b. ABSTRACT U	c. THIS PAGE U			19b. TELEPHONE NUMBER (Include Area Code) (937) 255-3636 x4709

THIS PAGE INTENTIONALLY LEFT BLANK